

UCSF

UC San Francisco Electronic Theses and Dissertations

Title

Chemical-Genetic Characterization of TORC2 in Yeast

Permalink

<https://escholarship.org/uc/item/3mb5352x>

Author

Kliegman, Joseph Ian Morningstar

Publication Date

2013

Peer reviewed|Thesis/dissertation

Chemical-Genetic Characterization of TORC2 in Yeast

by

Joseph Ian Morningstar Kliegman

DISSERTATION

Submitted in partial satisfaction of the requirements for the degree of

DOCTOR OF PHILOSOPHY

in

Biophysics

in the

GRADUATE DIVISION

of the

UNIVERSITY OF CALIFORNIA, SAN FRANCISCO

Copyright 2013

by

Joseph Ian Morningstar Kliegman

Acknowledgements

To Kevan Shokat for the freedom to explore my own ideas and for patience when they did not work.

To Nevan Krogan for upbeat, enthusiastic support and for the generous provisioning of bench space in support of my project.

To Jack Taunton for excellent scientific mentorship and critical conceptual review of my ideas and plan throughout graduate school.

To Arthur Glasfeld for the silver tongue that boosted me into the big leagues.

To William Draper and Mark DeWitt, my two best friends and fellow Biophysicists. While the three of us share deep loyalty and profound curiosity, I can only aspire to and be inspired by their genius.

To Alyssa Thunberg for being my rock and my light through the darkest time in graduate school.

To Julia DeWitt for giving me a piece of her boundless compassion and empathy and for getting me to the finish line.

To my parents Hanna and David Kliegman my most diehard fans for their blind optimism that I could get it done.

Most importantly, I would like to thank my sister, Sarah Kliegman, who paved the way and proved you could be born in a tipi and still end up with a Ph.D.

Abstract

As the clinical focus of cancer therapeutics shift from systemic toxins to targeted therapy, the ability to systematically identify promising candidates for multi-targeted cancer therapy is an increasing concern. Since screening for epistatic phenotypes offers a direct analog to the theoretical regimes used to evaluate synergistic activity of multi-targeted chemotherapy, high-throughput yeast genetics of the nutrient signaling pathway was explored in order to better characterize the signaling network, and discover candidates that synergize with the TOR kinase. Epistatic profiling of *S. pombe* and *S. cerevisiae* showed a high degree of network and functional conservation between the two species of yeast and to metazoans which was used to identify members of the TOR signaling network in yeast. Further, we developed the first method to selectively inhibit TOR complex 2 using pharmacology. We use this tool to profile the signaling network of TORC2 and show that this complex plays a regulatory role in the pentose phosphate pathway (PPP) that furnishes nucleotides and amino acids that are required for ribosome biogenesis.

Table of Contents

| | |
|-----------------------------------------------------------------------------------------------|-----------|
| Chapter 1: Introduction | 1 |
| Why targeted therapy | 1 |
| Why Target Kinases | 2 |
| Why multi-target therapy..... | 2 |
| How do we choose secondary targets..... | 3 |
| Difficulty of Systematic Screening | 4 |
| Common modes of action for combination Therapeutics | 5 |
| Importance of unbiased approaches to drug combinations..... | 7 |
| Chapter 2: Conservation of Genetic Interactions in Yeast | 11 |
| Introduction..... | 11 |
| Results and Discussion | 14 |
| A global genetic interaction map in <i>S. pombe</i> | 14 |
| A global map of functional modules in <i>S. pombe</i> | 16 |
| Network Interactions with TOR Pathway Genes..... | 19 |
| Interactions with TOR Pathway Genes | 21 |
| Identification of evolutionarily conserved functional modules | 24 |
| Network feature conservation | 27 |
| Hierarchical modularity of genetic interactions..... | 28 |
| Global connectivity of biological processes | 29 |
| Perspective | 30 |
| Methods | 33 |
| E-MAP data collection | 33 |
| Strain construction | 33 |
| Raw data collection..... | 33 |
| Scoring of genetic interactions..... | 33 |
| Chapter 3: Chemical-Genetics of Rapamycin Insensitive TORC2 in <i>S. cerevisiae</i> .. | 35 |
| Introduction..... | 35 |
| Results and Discussion | 38 |

| | |
|-------------------------------------------------------------------------|-----------|
| A chemical-genetic tool for studying TORC2 | 38 |
| A global map of genetic interactions with the TOR2 kinase | 44 |
| Characteristic dose dependent ChE-MAP interactions | 48 |
| Enrichment of Sphingolipid Biosynthesis in TORC2 ChE-MAP hits | 51 |
| Cellular Compartment and Process Enrichment of TORC2 Interactions | 53 |
| Integrated functional network of TOR signaling | 54 |
| Metabolomic analysis of TORC1 and as-TOR2 | 55 |
| Conclusions | 60 |
| Experimental Procedures | 62 |
| Generation of point mutants | 62 |
| E-MAP experiments | 63 |
| Dose-dependent interaction scoring system | 63 |
| Enrichment of TORC2 dose-dependent interactions | 64 |
| Tetrad Analysis | 64 |
| Spot Test Assay | 64 |
| Gene Ontology Network Analysis | 65 |
| Metabolite Measurement | 65 |
| Metabolic Flux Measurement | 65 |
| Appendix A: Chapter 2 Supplemental | 67 |
| Supplemental Tables | 67 |
| Supplemental Figures | 69 |
| Appendix B: Chapter 3 Supplemental | 70 |
| Supplemental Tables | 70 |
| Supplemental Figures | 71 |
| Bibliography | 75 |

List of Figures

| | |
|--------------------------------------------------------------------------|----|
| Figure 1. Theory of Genetic interactions | 12 |
| Figure 2. Conservation of Functional Genes | 15 |
| Figure 3. Hierarchical clustering of genetic interaction profiles | 18 |
| Figure 4. LAMTOR sequence alignment..... | 19 |
| Figure 5. Interaction hubs of TORC2. | 20 |
| Figure 6. Rad24 network topology | 20 |
| Figure 7. Model of rad24 interaction | 21 |
| Figure 8. Rad24 substrates and functional distribution | 23 |
| Figure 9. Enriched pathways in rad24 pulldown | 23 |
| Figure 10. Conserved Functional Modules | 26 |
| Figure 11. Modeling and Characterization of the as-TOR2 allele | 40 |
| Figure 12. Characterization of the as-TOR2 mutant..... | 42 |
| Figure 13. Chemical Epistasis Mapping of TORC1 and TORC2..... | 46 |
| Figure 14. Enrichment in Biological Processes | 52 |
| Figure 15. Effect of rapamycin and BEZ235 on metabolites in the PPP..... | 57 |
| Figure 16. Flux through the oxidative PPP..... | 59 |
| Figure S1. Compounds screened against as-alleles | 71 |
| Figure S2. Total Dose-Dependent ChE-MAP | 72 |
| Figure S3. ChEMAP parameters, plate pictures, and quantification | 73 |
| Figure S4. Regulation of metabolites..... | 74 |

Chapter 1: Introduction

As targeted chemotherapeutics become more widespread in clinical applications, the value and need for secondary targets that synergize for greater therapeutic efficacy will increase. Interest in the synergistic effect between two or more targets has led many clinicians and researchers to pursue polypharmacology—the simultaneous inhibition of several targets to achieve greater therapeutic efficacy. Clinical success using this strategy was first achieved with the combination of methotrexate and vincristine in the 1960s for treatment of childhood acute lymphoblastic leukemia and was subsequently extended to include other cancers (Chabner and Roberts, 2005). While many strategies have been used in attempts to identify synergistic effects between compounds, currently available systematic methods to predict high-value candidates are insufficient. The aim of this thesis is to explore the utility of high-throughput chemical genetics in selecting high-value candidates that could be used to develop combination chemotherapeutics.

Why targeted therapy

Molecularly targeted therapy takes advantage of the most recent advances in knowledge in cancer signaling and current tools to deliver a treatment that cures cancer more effectively with fewer side effects than more general alternatives (de Bono and Ashworth, 2010; Yap and Workman, 2012). Until relatively recently, drug treatment of cancer mainly involved cytotoxic chemotherapy that kills all rapidly dividing cells whether they were tumor or normal cells. The debilitating nature of this type of therapy is something researchers, physicians, and patients all have a strong interest in avoiding. As the mechanistic drivers of oncogenesis have been identified, it has become increasingly

possible to develop molecularly targeted therapies that selectively kill cancer cells over normal cells and avoid some of the most onerous side effects of cytotoxic therapy. Targeted therapeutics promise results with fewer side effects than cytotoxic alternatives and because of this are the primary focus of current and future drug development initiatives. Using a targeted approach, the most important challenge is to overcome solve the interrelated problems of genetic heterogeneity and drug resistance using intelligent drug combinations.

Why Target Kinases

Kinase inhibitors comprise one of the largest and fastest growing classes of new cancer drugs offering the greatest potential for effective polypharmacology. The focused effort on kinase drug development is not surprising considering kinases and their direct regulators comprise the most frequently mutated genes in cancer (Parsons et al., 2005; Wood et al., 2007). The success of targeting single kinases has been mixed due to rapidly emerging drug resistance and significant toxicity that limits the use of several of these agents to doses that do not block cancer growth (Boss et al., 2009; Haura et al., 2010). However, the majority of clinically successful drugs target multiple kinases (Knight et al., 2010; Mestres et al., 2009), suggesting that a multi-targeted approach using kinase inhibitors is a verified strategy.

Why multi-target therapy

While molecularly targeted therapies limit side effects, it has become apparent that a multi-target approach is more effective than selective targeting of a single oncogene. Initially, a single target approach was seen as promising due to the phenomenon of *oncogene addiction* wherein tumor cell survival becomes dependent on

overactive signaling of an oncogene and cells die when this signaling is reduced (Luo et al., 2009). However, further studies showed that single targeted therapy were more susceptible to common mechanisms of escape that allow the tumor cells to evade or evolve resistance to the therapy. These mechanisms include decreased metabolic activation or enhanced degradation of the drug, increased expression of the drug target, alteration of the target or pathway to reduce sensitivity, and reduced uptake of the drug (Brockman, 1963). More recently, deep sequencing has allowed characterization of extensive tumor heterogeneity that allows clonal evolution of resistant cells under the selective pressure of therapy (Gerlinger et al., 2012; Greaves and Maley, 2012). These genetically distinct drivers are able to substitute as the primary drivers of tumor growth when a targeted agent blocks growth of a subset of the tumor population. Newer, multi-targeted approaches take into account oncogene and nononcogene addiction, synthetic lethatities, and other pathway dependent vulnerabilities that can result in selective therapeutic effect on specific malignancies (de Bono and Ashworth, 2010; Yap and Workman, 2012). Multiple targets limit the ability of tumors to evade or evolve resistance to a given therapy.

How do we choose secondary targets

The full potential of multi-targeted cancer therapy will only be realized through identification of the best possible drug combinations. This will demand the use of emerging technologies such as next generation sequencing, systems biology, and novel computational approaches (Chen et al., 2012). To date the most common method employed to discover multi-targeted therapy regimes is by empirical testing of approved therapeutics in combination to see if there is some additive efficacy when the drugs are

dosed together. While this empirical strategy has led to several effective clinical combinations, the lack of a systematic approach makes progress toward future, potentially more efficacious combinations slow.

Sometimes selection is not rational at all, but due to serendipitous ‘off-target’ activity of a single chemotherapeutic. However, these off targets may act as secondary targets that contribute to therapeutic efficacy as is the case with Sorafanib (Wilhelm et al., 2006). Sorafanib was initially developed as a RAF kinase inhibitor, but its anticancer activity was later attributed to its inhibition of VEGFR2 and PDGFR (Ahmad and Eisen, 2004).

A new standard practice is needed for systematic identification of combination therapeutics that is sufficiently specific as to suggest likely targets for combination therapy while sufficiently general as to allow for collection and development of rules (selection criteria) for combination therapies.

Difficulty of Systematic Screening

Even screening combinations of approved therapies is difficult due to the scale of the challenge. To do a systematic screen of the approximately 250 small molecule anticancer agents that are currently approved, the total number of unique binary combinations (irrespective of dosing) is ~31,000. Systematically screening these binary combinations against a pre-defined set of tumor cell lines such as the NCI-60 tumor panel (Shoemaker, 2006) would increase the combinatorial complexity to almost 2 million distinct observations. For the approximately 1,200 compounds currently in development, the complexity rises to 720,000 binary combinations that would generate more than 43 million observations screened against the NCI-60 panel. Although not all of these

combinations make mechanistic sense, the complexity is further increased if nononcogene addiction, synthetic lethality, and other considerations are included in the analysis.

Another promising approach is *in vivo* phenotype based screening of whole organisms with potential chemotherapeutics. This type of approach for rational drug development combines the strengths of target and phenotype-based drug discovery (Dar et al., 2012). Dar and coworkers show that by tailoring the inhibition profile of a single chemotherapeutic while using a Ret-kinase driven model of multiple endocrine neoplasia in *Drosophila* to test their results, they could optimize the inhibition strategy to rescue oncogenic lethality and avoid reduced efficacy and enhanced toxicity of closely related Ret inhibitors. This type of *in vivo* screening could be used to great effect to test hypotheses derived from high throughput screening performed *in vitro* or in more distant model organisms.

A key need, therefore, are systematic methods to evaluate and prioritize the best potential combinations for testing using an intelligent combination of computational and experimental biology, pharmacology, and high throughput technologies (Hawkins et al., 2010; Iadevaia et al., 2010).

Common modes of action for combination Therapeutics

There are several potential approaches to the rational selection of drug targets based on specific mutations, or their roles in the cell as central signal integrators for several pathways that promote oncogenic signaling. If a rational selection is made, once a target is selected, there are typically only a few structural approaches to maximize the

combined therapeutic of the second target. These approaches can be roughly referred to as *same target inhibition*, *vertical inhibition*, and *horizontal inhibition*.

Same target inhibition typically refers to inhibiting the same target with multiple drugs. For example, an antibody therapy to a receptor tyrosine kinase (RTK) can be combined with a kinase inhibitor to achieve more complete inhibition of the RTK signaling. The definition can be broadened to include inhibition of several targets that share the same function. A good example of this mode of combination therapy is with oncogenic receptor tyrosine kinases (RTKs). Activation of oncogenes and inactivation of tumor suppressor genes downstream of RTKs leads to activation of oncogenic signaling. Efficacy of targeted therapies can be enhanced, or resistance can be overcome by simultaneous targeting of multiple RTKs.

Combinatorial targeting within a linear oncogenic pathway is called vertical inhibition. Vertical inhibition could include the receptor at the start of the pathway and a signaling checkpoint downstream of the receptor. Due to the fact that the androgen receptor pathway remains the main oncogenic driver in metastatic castrate-resistant prostate cancer (de Bono et al., 2011), the successful clinical intervention using the CYP17 inhibitor abiraterone and the potent androgen receptor antagonist enzalutamide demonstrates the efficacy of vertical inhibition. In addition to the fact that vertical inhibition is a verified strategy for cancer treatment, it is also an easily testable phenotype in genetic and chemical genetic screening. This screening can be performed in high-throughput fashion in model organisms and allows the vertical interaction between targets (often referred to as a linear, buffering, or positive interaction) to be identified.

In contrast, horizontal inhibition entails combinatorial targeting of parallel oncogenic signaling pathways to affect a synthetic lethal phenotype on inhibited cells. An example of clinical pursuit of a horizontal inhibition strategy is based on the observation that phosphorylation of AKT increases when inhibitors of a kinase acting in a parallel pathway (MEK) is inhibited. Preliminary efficacy of the combination of a MEK inhibitor (AZD6244) and an allosteric AKT inhibitor (MK2206) has been shown in NSCLC cancer in ongoing clinical trials. Horizontal inhibition also forms the basis for phenotype based high-throughput screening. In these screens horizontal interactions are referred to as synthetic/sick, parallel, or negative interactions between targets.

Regardless of the rational logic of multi-targeted inhibition, the most important problem to overcome is the additive (or in some cases multiplicative) toxicity of the combination that can lead to clinical failure. This increased toxicity led to the notable failure of bevacizumab and sunitinib (both VEGF targeting agents), which in combination lead to hypertension and hemolytic anemia (Moroney et al., 2010). In contrast, the combination of BRAF (GSK2118436) and MEK (GSK1120212) inhibitors in a vertical inhibition scheme leads to acceptable levels of toxicity, high clinical efficacy, and avoids a well characterized mechanism of resistance to BRAF inhibition resulting in paradoxical activation of CRAF in healthy cells following treatment (Heidorn et al., 2010; Poulikakos et al., 2010).

Importance of unbiased approaches to drug combinations

The most effective approach toward identification of novel combination therapies are unbiased screening strategies. These strategies provide an important complement to hypothesis driven and empirical approaches to identify new, potentially effective drug

combinations. The two most frequently employed techniques for unbiased target screening are multi-drug screens on cultured cells, and genome-wide loss or gain of function screens in tumor cells where gain or loss of function can identify genes that confer sensitivity or resistance to chemotherapy.

Combination screening of licensed drugs using high-throughput methods can be used to great effect to identify synergistic interactions with clinically available compounds (Keith et al., 2005). Such screening uncovered that the combination of the antiparasitic agent pentamidine and the antipsychotic chlorpromazine result in synergistic effect in preventing cancer cells from undergoing mitosis. Similarly, an unbiased RNAi screen identified feedback activation of EGFR as a cause of resistance of colon cancer cells to BRAF inhibition. These data suggest the use of BRAF and EGFR inhibitors in BRAF mutant cells that overexpress EGFR may be a good treatment strategy for colon cancers (Prahallad et al., 2012).

The objective of unbiased screens should be to construct a human cellular wiring map that can model aberrant signaling phenomenon that result from cancer and suggest multitarget intervention strategies based on computational overlay of available therapeutics and drugs that are in development. While this goal is years off by any measure, a goal that is tractable with current methods and techniques is high throughput chemical genetic screens in model organisms and using evolutionary conservation among pathways and processes to infer functional connections in higher organisms. Further, these methods can offer a first look at synergistic interactions that result from chemical or genetic knockdown of cellular components.

Determining synergy for a chemical genetic phenomenon is complicated since historical precedent uses different models to evaluate the null-interaction or non-interacting genes in a biological context. While genetic interaction models typically rely on a multiplicative model to evaluate non-interacting genes (Bliss independence, cite), chemical interaction models typically rely on additive models (Lowe additivity, cite), which is the dose-additive expectation for a drug added to itself. To account for this controversy we have adopted a hybrid theory for chemical-genetic interactions in our study that incorporates a multiplicative model following Bliss independence in combination with a null-effect reference containing no chemical perturbation.

We have undertaken several approaches to combination chemical-genetics. A forward genetic screen in *S. pombe* allowed us to characterize the effect of known human TOR inhibitors for their conserved behavior. Incorporation of these strains into a genetically robust species cross-comparison of double mutants across the genome allowed us to map the network connectivity and characterize the functions of previously unannotated genotypes that play important roles in TOR signaling.

Further, we endeavor to create a generalizable platform with which researchers may systematically study synergistic interactions in combination with predefined therapeutic targets. This platform is sufficiently broad and unbiased and has the capability to identify novel targets and novel pathways that work in concert or communicate with the predefined therapeutic target. The platform is also sufficiently specific that it reports on the catalytic activity of the enzyme involved rather than reporting on secondary consequences of the technique such as destruction of a protein complex or the loss of a scaffolding interaction.

In this dissertation, we have applied the tools of yeast genetics and chemical biology to the problem of finding high-value secondary targets to be used in combination with TOR inhibitors that are currently in development as therapeutics. Our approach simultaneously offers new evidence toward signaling roles that TOR plays in the cell and offers interesting targets both in horizontal and vertical inhibition schemes that may have high potential as combination therapeutics.

Chapter 2: Conservation of Genetic Interactions in Yeast

Introduction

The genetic equivalent of synergistic drug interactions is the phenomenon of epistasis. Epistasis occurs when the phenotype of one gene is affected by the presence or absence of another gene, relationships that are termed genetic (or epistatic) interactions (GIs). Unlike protein-protein interactions (PPIs), which are limited to gene products that physically interact, GIs report on functional relationships, and reveal how groups of proteins work together to carry out high level biological functions and describe the cross-talk between pathways and processes (Beltrao et al., 2010). Thus, GI networks are a natural complement to PPI maps and integrating these two types of information has proven to be extremely powerful in understanding complex biological phenomenon in a variety of systems (Bandyopadhyay et al., 2008; Collins et al., 2007; Hannum et al., 2009; Kelley and Ideker, 2005; Keogh et al., 2005; Wilmes et al., 2008).

Since genetic interactions serve as a bridge between genotype and phenotype, they are instrumental in revealing functional redundancies in biological networks. For example, in *S. cerevisiae*, only ~1100 individual gene deletions are lethal in rich media (Giaever et al., 2002) while ~11,000 pairwise deletions have been reported to cause cell death (Stark et al., 2011). It has been suggested that genetic interactions are vital to understanding the causes of human disease (Lehner, 2007). The combination of these tools with targeted chemistry may be even more vital in uncovering secondary targets for chemotherapeutic development.

Genetic interactions can be divided into three broad categories: 1) aggravating (negative), where the phenotype is stronger than is expected from the phenotypes

associated with the single perturbations; 2) alleviating (positive), where the compounded phenotype is weaker than anticipated and 3) neutral, where the measured phenotypic consequence is as expected (Figure 1) (Beltrao et al., 2010; Phillips, 2008). Frameworks for modeling and scoring genetic interactions are normally centered at zero (i.e. neutral interactions) (Baryshnikova et al., 2010; Collins et al., 2010; 2006; Horn et al., 2011; Schuldiner et al., 2005) and have been developed to capture a continuous spectrum of phenotypic strengths. The bulk of the available data has been generated in the budding yeast, *S. cerevisiae*, where fitness (often derived from colony size) is the most commonly used as a phenotypic readout. Several methodologies have been developed to identify and quantify these relationships in a variety of other organisms, including *E. coli* (Butland et al., 2008; Typas et al., 2008), *S. pombe* (Dixon et al., 2008; Roguev et al., 2007), *C. elegans* (Byrne et al., 2007; Lehner et al., 2006) and *D. melanogaster* (Horn et al., 2011), by either deleting, mutating or knocking down expression of genes in a pair-wise fashion.

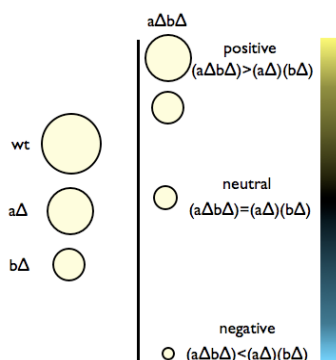


Figure 1. Theory of Genetic interactions

Growth phenotypes at left can interact neutrally, positively, or negatively.

To date, genome-wide epistasis data has only been available for *S. cerevisiae* (Costanzo et al., 2010). In other organisms, the available datasets are either small in scale (Tischler et al., 2008) or focused on specific processes or pathways, including an analysis of chromatin function in *S. pombe* (Roguev et al., 2008), cell envelope biogenesis in *E.*

coli (Babu et al., 2011), and signaling networks in *D. melanogaster* (Horn et al., 2011) and *C. elegans* (Byrne et al., 2007; Lehner et al., 2006). Therefore, the extent to which genetic interactions are conserved across species remains an open question. While earlier work has reported specific trends relating to the conservation and evolution of GIs (Byrne et al., 2007; Dixon et al., 2008; Roguev et al., 2008; Tischler et al., 2008), it is not clear how much of the knowledge learned in one species can be applied to others and which individual interactions and network features are likely to be conserved.

In this study, we present a genome-wide, quantitative genetic interaction map (or E-MAP) for the fission yeast, *S. pombe*. It is estimated that *S. pombe* diverged from *S. cerevisiae* ~400 million years ago (Sipiczki, 2000) and in many ways is more similar to metazoans, including with respect to mRNA splicing (due to the extensive presence of introns), gene expression controlled in part by the RNAi machinery, metazoan-like epigenetic mechanisms, and cell cycle regulation by the G2/M transition control (Sunnerhagen and Piskur, 2010).

Our data allows for a comprehensive functional interrogation of these (and other) biological processes and facilitated the creation of a global *S. pombe* map of functional modules and assignment of specific function to many previously uncharacterized genes. Finally, comparing these data to a newly consolidated GI map from *S. cerevisiae* has allowed for an unprecedented comparison of the genetic architecture of two organisms, revealing global trends that arguably exist in all eukaryotic species (Ryan et al., 2012). These global trends support the generality of potential secondary therapeutic targets for higher organisms derived from experimental results from organisms that do not suffer from cancer.

We give special attention in our analysis of this large dataset to the Target of Rapamycin (TOR) since it is an *essential* control point in cancer that plays a role in cancer progression. Discovering epistatic interactions with this complex and proving a high degree of network conservation between organisms provides strong evidence that could greatly aid the development of synergistic therapeutics.

Results and Discussion

A global genetic interaction map in *S. pombe*

Krogan and coworkers developed a system, termed PEM (Pombe Epistasis Mapper) (Roguev et al., 2007), which allows for the systematic creation of double mutants in fission yeast using a high-density, plate based assay. Using the PEM technology, we screened 953 alleles (Appendix A, Table S1) of 876 genes against a fission yeast mutant library containing more than 2000 deletions (Appendix A, Table S1), including tens of queries specifically related to the TOR signaling pathway (Table S4) resulting in ~1.6 million pairwise measurements (Appendix A, Datasets S1, S2, S4). The majority of the genes screened are broadly conserved across eukaryotes, with subsets that are fungi- and fission yeast-specific (Figure 2A; Appendix A, Table S1). Using all of the individual genetic interactions for each mutant, we obtained interaction profiles for ~50% of the genome, resulting in representation of over half of the non-essential components of virtually every major biological process (Figure 2B; Appendix A, Table S2). Both internal and external validation showed the data to be of high quality and reproducibility. All genetic interaction data is included in a searchable and interactive website (<http://interactome-cmp.ucsf.edu/pombe2012>).

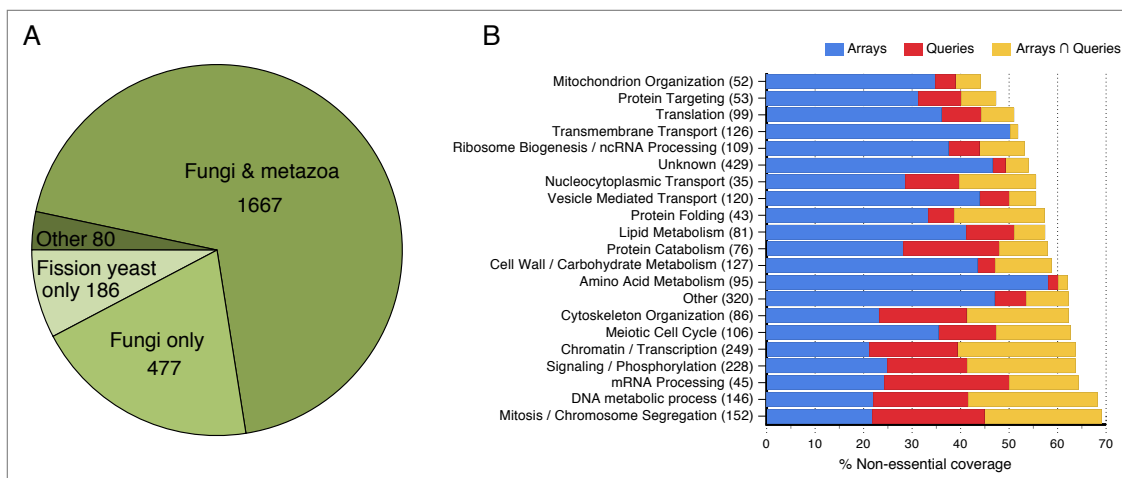


Figure 1

Figure 2. Conservation of Functional Genes

(A) Species distribution of the genes in the fission yeast E-MAP. For a complete list of the genes in each category, see Table S1 (B) Coverage of the non-essential genes genetically analysed in this study with respect to different biological processes. Shown are genes present on the library array from Bioneer (<http://pombe.bioneer.co.kr/>) only (blue), as queries only (red) and present as both arrays and queries (orange). For each process, the total number of non-essential genes present in the E-MAP is given as the figure in brackets. For a full assignment of genes to different biological processes, see Table S3

A global map of functional modules in *S. pombe*

Krogan and coworkers previously reported that pairs of genes with similar genetic interaction profiles frequently encode proteins that belong to the same protein complex or work in the same functional pathway in fission yeast (Roguev et al., 2008), a network feature also observed in *S. cerevisiae* (Beltrao et al., 2010; Collins et al., 2007; Schuldiner et al., 2005; Tong et al., 2004). In attempt to represent the entire dataset in an intuitive fashion, the profile from each mutant was compared to the profiles of all other mutants on the E-MAP and a similarity score was generated for each pair of mutants (Appendix A, Dataset S3). These similarity scores were then subjected to hierarchical clustering (Appendix A, Dataset S4), grouping genes that have similar genetic interaction profiles, suggesting that they are functionally related and/or their protein products are physically associated (Figure 3). Many known protein complexes were recapitulated from this matrix, including the SWR-C chromatin-remodelling complex (Kobor et al., 2004; Krogan et al., 2003; Mizuguchi et al., 2004), CTDK-C (Sterner et al., 1995) and the GCN5 module of SAGA (Helmlinger et al., 2008), complexes that regulate transcription by RNA polymerase II, the retromer complex (Iwaki et al., 2006; Seaman et al., 1998), as well as the large and small components of the ribosome (Figure 3). Protein complexes whose subunits are entirely essential in *S. cerevisiae*, and thus difficult to genetically interrogate in that organism, were also identified, including the chromosome segregation complex, DASH-C (Figure 3). Interestingly, subunits of DASH-C clustered with the kinesins *klp5* and *klp6*, whose protein products form a heterocomplex (Garcia et al., 2002) which functionally overlaps DASH-C in establishing bipolar chromosome attachment during mitosis (Sanchez-Perez et al., 2005). *dad1* has a lower similarity score

to other members of DASH-C (Figure 3), consistent with its unique role as a constitutive component of the kinetochore (Sanchez-Perez et al., 2005).

As genetic data allows for the grouping together of factors that work together but are not necessarily physically associated, we were also able to identify several previously characterized functional pathways. These included components of RNAi pathway, the AP3 adaptor complex with *vam7*, components of the DNA damage checkpoint pathway and factors involved in protein glycosylation and TOR signaling (Figure 3). The TOR pathway in fission yeast, like that in higher eukaryotes, has a tuberous sclerosis complex composed of *tsc1* and *tsc2* that acts as a regulator for TOR signaling. In contrast to its regulatory role on TOR Complex 1 where TSC negatively regulates TOR via GTPase RHEB, the TSC complex has been shown to be necessary for activation of TOR Complex 2 in mammalian cells (Huang et al., 2008). Consistent with this role, *tsc1* and *tsc2* group together with members of the TORC2 complex, including *tor1* and *tsc11* (Figure 3). Within the TORC2 group is the uncharacterized gene SPBC1778.05c, which shows high sequence similarity (39%) (Figure 4) with the human gene LAMTOR—a factor known to regulate the Tor pathway (Sancak et al., 2010). This high sequence similarity and our genetic evidence linking SPBC1778.05c to the TOR pathway, suggests that this gene is the *S. pombe* LAMTOR2 ortholog.

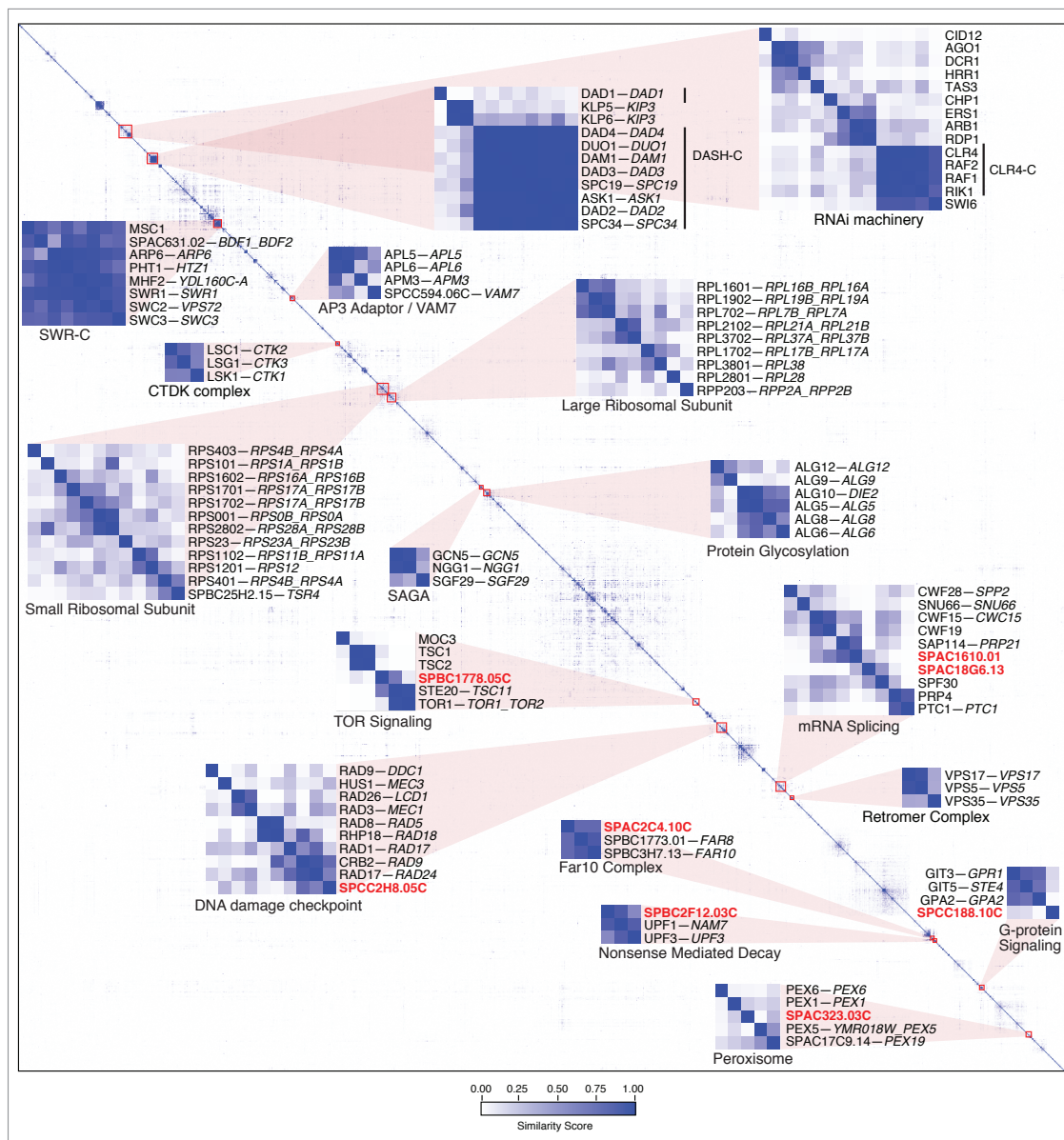


Figure 2

Figure 3. Hierarchical clustering of genetic interaction profiles

Genes are grouped based on the similarity of their genetic interaction profiles. Modules discussed in the text are magnified and labeled and uncharacterized genes within these modules are highlighted in bold red. Genes are labelled using their *S. pombe* common name, followed by the common names of their *S. cerevisiae* orthologs if present (with paralogs separated by underscores). Only genes with at least one similarity score ≥ 0.1 are included in this representation, however the similarity scores for all gene pairs are provided in Dataset S3 and the Treeview file used to create this figure is in Dataset S4.

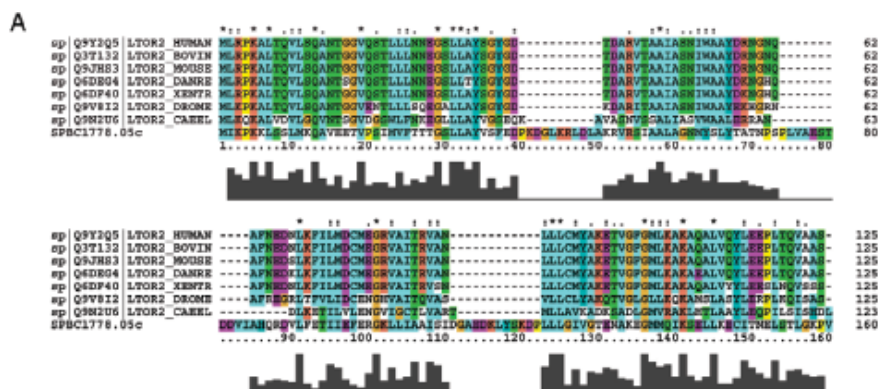


Figure 4. LAMTOR sequence alignment

Protein sequence alignment shows high sequence conservation between mammalian LAMTOR and *S. pombe* ortholog, particularly in structured regions of the protein.

Network Interactions with TOR Pathway Genes

To analyze the results of the screen, we conducted network analysis to reveal genes that behave as signaling hubs in the TOR network (Figure 5). These genes show enrichment for significant genetic interactions above and were used to generate characteristic networks showing the genes in the interaction hubs

The interaction network between *gad8*, and the *tsc* complex offers confirmation that the technique is reporting interactions in accordance with expectations but also facilitates new observations. The nucleus of this network is *gad8*, a well-characterized substrate of TORC1 that is functionally equivalent to SCH9 in *S. cerevisiae* or S6K in mammals (undefined author et al., 2008). Interestingly, a cluster of genes show strong positive interactions with *gad8*, *tsc1*, and *tsc2*, while other genes show strong negative interactions with *tsc1* and *tsc2*, but no interaction with *gad8*. This suggests that among genes that function in pathway with the *tsc* complex are also in pathway with *gad8*, however genes acting in a parallel pathway do not functionally interact with outputs of TORC1.

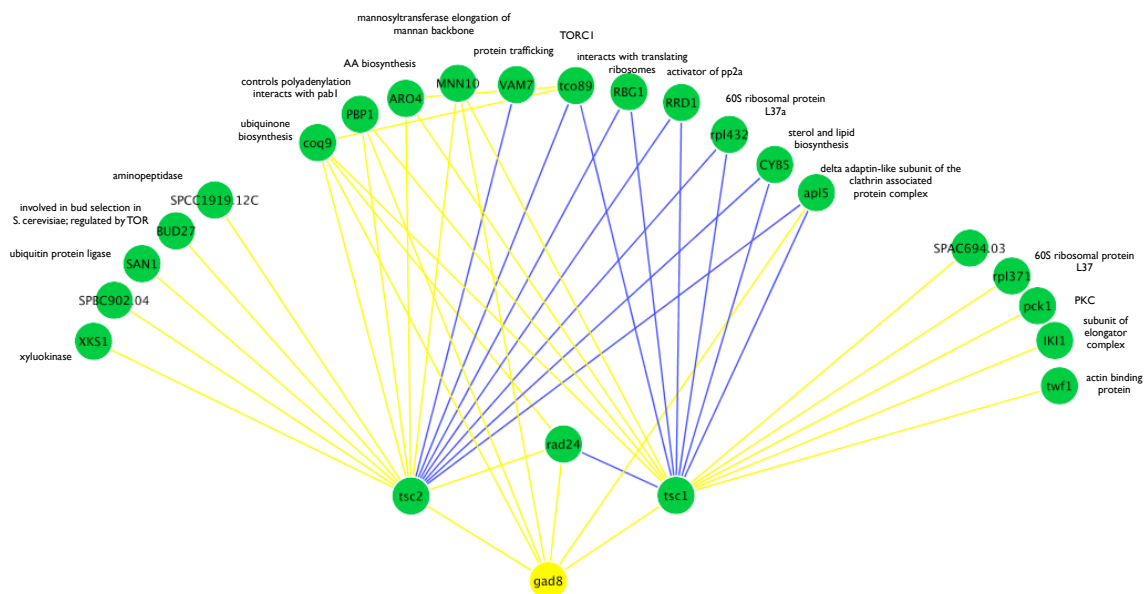


Figure 5. Interaction hubs of TORC2.

Shows functional interactions between the highest correlation-coefficient hubs in the TOR pathway (*tsc1*, *tsc2*, *gad8*, *rad24*), and those discovered in the genome wide screen.

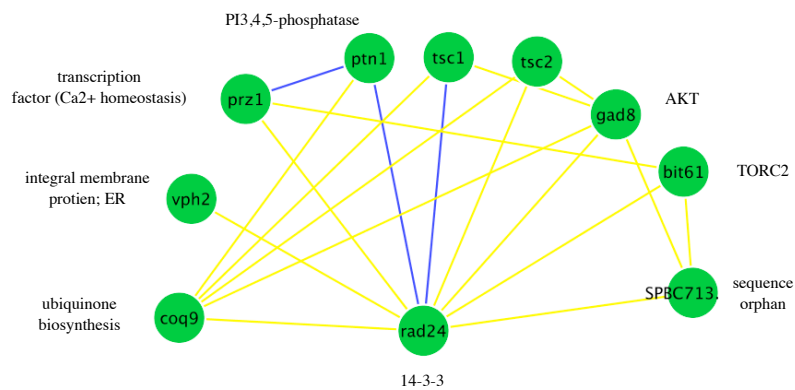


Figure 6. Rad24 network topology

Rad24 had the most interconnected network topology with TORC1 and TORC2 components. Positive interactions are in yellow, negative interactions are in blue.

Interactions with TOR Pathway Genes

Strong interactions with previously annotated TOR pathway genes and interconnected network topology were the primary criterion used to evaluate hits for further follow up. The most interconnected hit among TORC1 and TORC2 genes was rad24 (Figure 6).

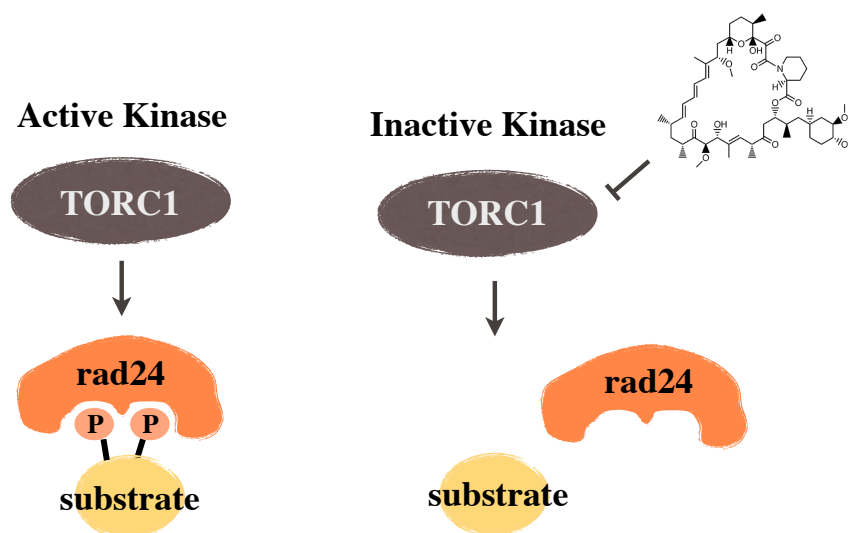


Figure 7. Model of rad24 interaction

When TORC1 is active rad24 binds its substrate and represses its activity, when TORC1 is inactive or inactivated using rapamycin, the TORC1 substrate goes unphosphorylated and does not bind rad24.

We hypothesized that rad24 could be used as a proxy for activity by TORC1 based on the known function of rad24 (and rad25) as 14-3-3 proteins. 14-3-3 proteins are regulatory proteins that typically bind phosphorylated substrates in a bidentate fashion. We reasoned that if TORC1 was active, rad24 would bind its substrates which could be pulled down with an epitope-tagged rad24. However, if TORC1 was inactivated using

rapamycin, rad24 would not associate with its substrates and they would not be pulled down (Figure 7).

A pulldown of epitope-tagged rad24 showed the protein was expressed at markedly different levels in concentration normalized lysates. The eluent of the pulldown was run on a silver stained gel and digests characterized using mass spectrometry showed an enrichment of peptides from ribosomal genes and peptides in glycolysis with a higher number of binding partners identified in the rapamycin treated compared to the untreated samples (Figure 8). Based on the positive genetic interactions observed with members of TORC2 and the abundance of evidence for feedback activation of the pathway upon rapamycin treatment (Sun et al., 2005) we propose this increase in binding partners of rad24 could be due to feedback activation of the pathway and/or compensation by TORC2. Results show the greatest changes to rad24 substrate binding induced by rapamycin occur in the pentose phosphate pathway (PPP) and in glycolysis (Figure 9). The increase in binding partners in the PPP and glycolysis makes sense given the central role of TOR as an integrator of nutrient signaling.

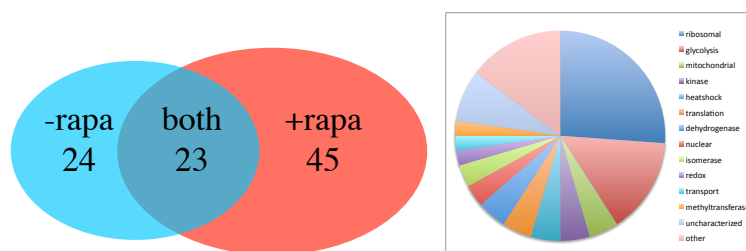


Figure 8. Rad24 substrates and functional distribution
Substrates of rad24 identified in triplicate measurement of untreated, treated, and found in both samples. Functional distribution of identified binding partners shown (right).

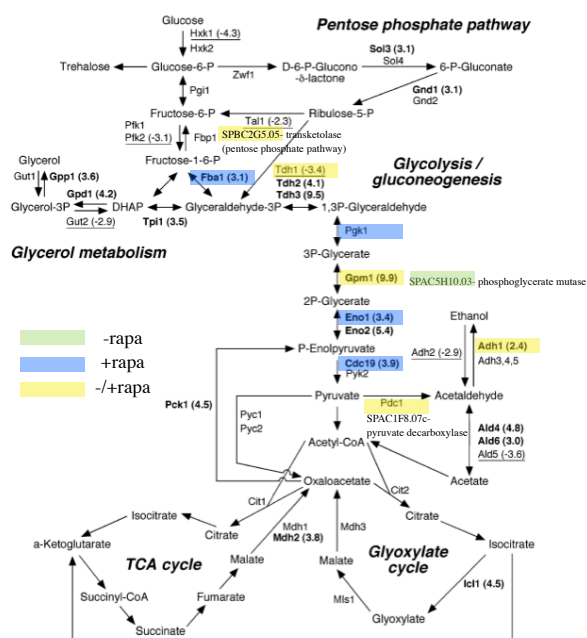


Figure 9. Enriched pathways in rad24 pulldown
Glycolysis and gluconeogenesis were the most highly enriched pathways in samples treated with rapamycin.

Identification of evolutionarily conserved functional modules

To date, large-scale, quantitative genetic interaction data has only been collected in *S. cerevisiae*. However, the *S. pombe* dataset described in this study is the largest genetic interaction map generated in a species other than budding yeast, data that can allow, for the first time, an evolutionary analysis of the genetic architecture of two eukaryotic species. The utility of cross-species comparison of functional modules extends to using functional genetics experiments to predict secondary targets that could be interesting targets for cancer therapy.

To facilitate this extensive cross-species analysis, we use a novel algorithm to integrate all existing quantitative genetic interaction data from *S. cerevisiae* into one dataset, including data from a recent genome wide screen (Costanzo et al., 2010) and 10 smaller scale functionally focused E-MAP screens (Aguilar et al., 2010; Bandyopadhyay et al., 2010; Collins et al., 2007; Fiedler et al., 2009; Hoppins et al., 2011; Schuldiner et al., 2005; Wilmes et al., 2008; Zheng et al., 2010). The scoring system used to generate the genome wide dataset (SGA-score (Baryshnikova et al., 2010)) differs from that used to generate the functionally focused E-MAP datasets (S-score (Collins et al., 2010)), although both methods attempt to model the same biological phenomena.

Ryan and coworkers first verified that the genome wide data was of similar quality to the functionally focused screens in terms of internal reproducibility, ability to predict known genetic interactions and using the similarity of genetic interaction profiles' ability to predict protein-protein interactions. It verified that the genetic interaction scores from both methods were highly correlated. Despite this high correlation, the range and distribution of interaction scores from both methods was significantly different. In order

to overcome these differences, a non-linear scaling method was applied to the SGA data and this scaled dataset and the collated E-MAP datasets (Appendix A, Dataset S2) were merged into a single dataset (Appendix A, Dataset S4).

The identification of conserved biological networks is a growing field of research (Sharan and Ideker, 2006). For example, methods have been developed to identify conserved linear pathways (Kelley et al., 2003) or protein complexes (Sharan et al., 2005) from protein interaction networks, or conserved co-regulated modules from gene expression (Stuart et al., 2003) or chromatin immunoprecipitation data (Tan et al., 2007). However, this work is the first global attempt to use genetic interaction profiles to identify conserved modules across species. Using a newly developed clustering procedure designed specifically to identify conserved functional modules from genetic interaction data, 105 evolutionarily conserved functional modules present in both species were identified (Figure 10). Gene Ontology (GO) analysis indicated that 61 of them are significantly enriched for known complexes, including the mitotic checkpoint complex (*mad1*, *mad2*, *mad3*, *bub3*) (Fraschini et al., 2001), or pathways, such as the *alg* genes involved in oligosaccharyl synthesis (*alg5*, *alg6*, *alg8*, *alg9*, *alg12*, *die2*) (Jakob, 1998). A literature survey of the remaining 44 modules revealed that, although not documented in the Gene Ontology, many of them belong to the same pathway or complex, including the Tma20/Tma22 translation complex (Fleischer et al., 2006) and Aim13/Fcj1 (Figure 10), which is part of the recently discovered MitOS complex (Hoppins et al., 2011).

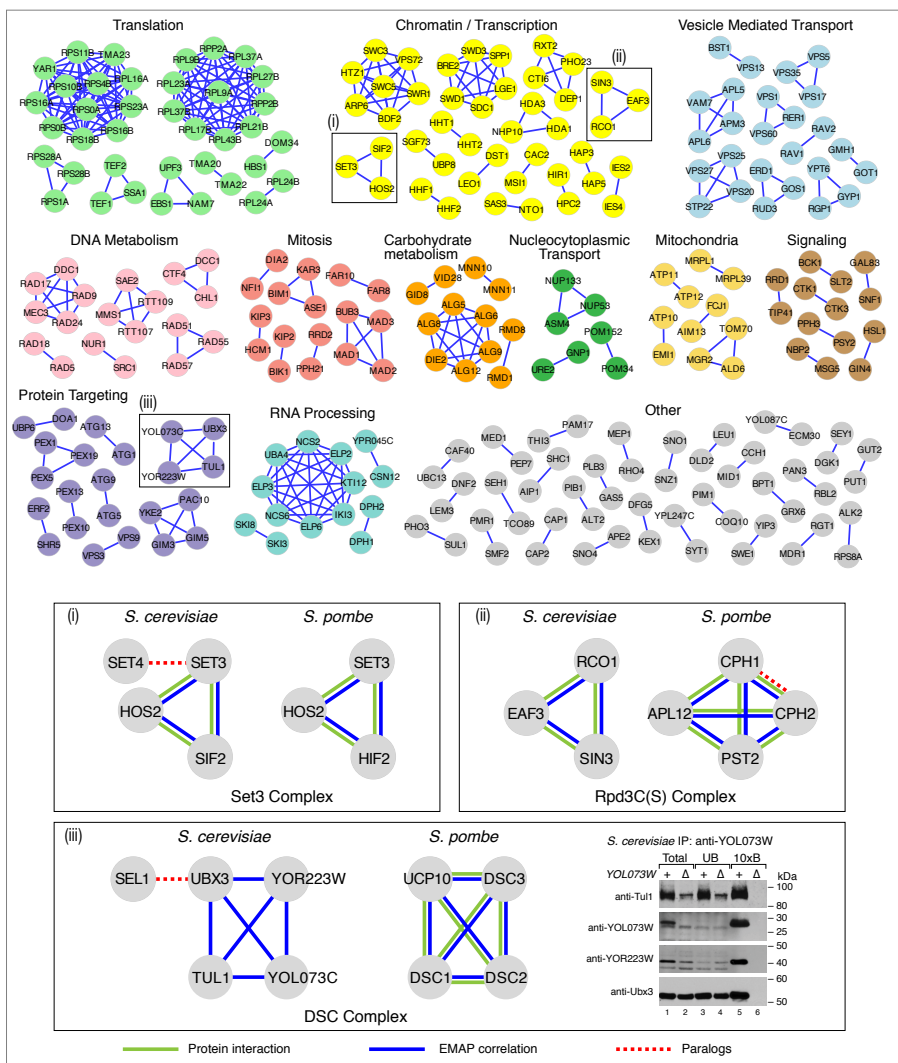


Figure 4

Figure 10. Conserved Functional Modules

Groups of genes with highly correlated genetic interaction profiles in both *S. pombe* and *S. cerevisiae* are shown. *S. cerevisiae* gene names were used for labeling, as many of the *S. pombe* orthologs lack common name. Modules are manually grouped and colored according to the biological process they are involved in. Modules from the insets are boxed and correspond to the Set3 complex (i), the Rpd3C(S) (ii) and the DSC complex (iii). A full list of the modules identified, and their *S. pombe* counterparts, is given in Table S2. For the immunoprecipitation assay in (iii), Dsc2 binding proteins were immunopurified from detergent lysates of wild-type and *dsc2Δ* cells using anti-Dsc2 affinity purified polyclonal antibody. Equal amounts of total (lanes 1 and 2) and unbound fractions (lanes 3 and 4) along with 10× bound fractions (lanes 5 and 6) were immunoblotted using the indicated HRP-conjugated antibodies. Blue edges correspond to pairs of genes that have high E-MAP correlations, green edges represent pairs of factors that are physically associated from previous studies whereas dashed red edges represent paralogs within one species (Ryan et al., 2012).

Network feature conservation

By comparing genetic interaction data derived from *S. cerevisiae* to other, orthogonal datasets, several interesting trends have been previously reported. For example, pairs of genes that display strong genetic interactions are significantly more likely than random gene pairs to share other biological features, such as similar deletion phenotypes (Tong et al., 2004), membership of the same biological process (Wilmes et al., 2008), and, particularly in the case of positive interactions, membership of the same protein complex (Collins et al., 2007; Schuldiner et al., 2005). This was confirmed by Ryan and coworkers (2012), suggesting the complexes would also be present in other eukaryotic species. Additionally, genes whose products are members of protein complexes display a disproportionately high number of genetic interactions (Michaut et al., 2011) and we find this network topology feature conserved in both *S. cerevisiae* and *S. pombe*.

We also probed two classes of genes: sequence orphans and ortho-essential genes (e.g. genes non-essential in one species and essential in the other). We find that in both species, sequence orphans have significantly fewer genetic interactions when compared to other genes. These results are consistent with either of the two predominant interpretations for the existence of sequence orphans. First, the orphans are rapidly evolving, preventing the identification of a sequence ortholog, and the lack of genetic interactions represents a lack of functional constraints from other genes. A second explanation is that they have arisen *de novo* from non-coding regions and the lack of interactions indicates that they have not yet been fully integrated into the cellular network, a theory consistent with observations from protein-protein interaction networks (Capra et al., 2010).

Finally, in the two yeast species, 83% of the one-to-one orthologs have conserved dispensibility – they are essential or viable in both species (Michaut et al., 2011). We find that the remaining 17% (ortho-essential genes) have ~2.5 times more than average genetic interactions, suggesting that, although they are no longer essential for growth under standard laboratory conditions, they still contribute significantly to the robustness of the cell. Since we have observed many global genetic trends conserved in these two very divergent organisms, we suggest that they ultimately will be present throughout all eukaryotic species.

Hierarchical modularity of genetic interactions

Previous work has shown that the genetic interactions between components of protein complexes, especially positive interactions, are highly conserved between budding and fission yeast (Roguev et al., 2008). The data presented here support and expand these observations. To make our conservation calculations as accurate as possible, they were adjusted to take into account the reproducibility of different categories of interactions (Appendix A, Table S3). In addition to high conservation of positive genetic interactions within protein complexes (70%) (S-score > 1.8), we find a high degree of conservation for negative interactions (68%) (S-score < -2.3). This new finding suggests that not just the dependencies, but also the buffering relationships within complexes are highly conserved. These findings are consistent with data from other experimental methods suggesting that protein complexes are highly conserved across species (van Dam and Snel, 2008).

However, biological systems do not exhibit just one level of modularity, since groups of complexes and pathways function together to carry out highly orchestrated and

complex cellular processes such as translation or mitosis. Indeed, upon careful scrutiny of the data presented in Figure 10, many instances of such hierarchical modularity can be found. For example, we identify two distinct clusters corresponding to the large and small ribosomal subunits, which are ultimately united in a single ‘ribosomal’ subtree (Appendix A, Figure S1). Moving higher up the tree reveals an even larger cluster encompassing many genes involved in translation regulation and ribosome biogenesis (Figure S1).

Interestingly, using S-score cut-offs described above and process definitions obtained from the gene ontology (Appendix A, Tables S3), we find that interactions between genes belonging to the same biological process are less conserved than interactions within complexes (positive interactions: 58%; negative interactions: 38%), but significantly more conserved than interactions between genes functioning in separate processes (positive interactions: 19%; negative interactions: 15%). Analysis of the complete dataset is consistent with these observations: the genetic data between the two species becomes less conserved as larger modules are considered (same complex: $r=0.46$; same process: $r=0.16$; different process: $r=0.03$). These observations, combined with the fact that genes within the same complex or process are significantly more likely to interact than random gene pairs, suggests that biological systems exhibit multiple levels of modularity and that the rate of rewiring of genetic interactions is dependent on the specificity of the module they belong to.

Global connectivity of biological processes

Functional connectivity also exists between the different processes in the *S. pombe* and *S. cerevisiae*. The role of chromatin as a ‘hub process’ has previously been identified in a genome wide *S. cerevisiae* genetic interaction map (Costanzo et al., 2010)

and is also supported by smaller scale screens from *C. elegans*, suggesting that it may be a common feature of eukaryotic genetic interaction networks (Lehner et al., 2006). Conversely, we see that some processes, such as Amino Acid Metabolism and Transmembrane Transport, have very few genetic interactions, suggesting less cellular information is being passed through them, at least under the conditions used to collect the data.

Comparison of E-MAPs in *S. pombe* and *S. cerevisiae* shows that at a global level, both organisms share remarkable similarities and the level of cross-talk between distinct biological processes highly conserved (Ryan et al., 2012). Several of the processes that show conserved genetic links are expected, including DNA metabolism with Mitosis/Chromosome Segregation and Translation with Ribosome Biogenesis/ncRNA Processing. However, more intriguing connections also exist, including a link between Mitosis/Chromosome Segregation and mRNA Processing (Murakami et al., 2007; Tang et al., 2011). While further work will be required to understand the molecular mechanisms that link these different processes, the evolutionary conservation between both *S. pombe* and *S. cerevisiae* suggests that these links are likely to exist in other, potentially higher, eukaryotic organisms.

Perspective

By any rational standard, designs in biological systems are very complex and incredibly efficient. In the formal engineering and systems design sense, however, biological designs are not optimal (Kashtan and Alon, 2005). Indeed, the ability of the budding yeast to withstand perturbations to ~80% of its genes under standard laboratory conditions suggests that it has an excess of components, and is not optimized for

performance, at least under these conditions. However, outside of the laboratory, living systems must survive in a wide range of conditions, and be robust to a wide variety of mutations. Despite, and perhaps because of that, biological systems can achieve optimization or near optimization within defined constraints provided that there are limits on range of environmental conditions and possible designs. However, high level of optimization for any single task under specific conditions renders a system extremely fragile and vulnerable to change (Kitano, 2010). Hence, the designs observed in biological systems are merely a generic solution satisfying a subset of constraints and extreme degrees of optimization for a particular set of parameters are rarely observed. This lack of optimization makes biological systems very flexible, adaptable, robust and perhaps most importantly, evolvable.

Our work and the work of Ryan and coworkers (2012) shows a hierarchical model of evolutionary conservation within genetic interactions networks. There appears to exist different constraints on the evolvability of different parts of the system. This is reminiscent of the concept of ‘coupling’ in software development and systems design, a measure of the degree to which different components of the system depend on each other to function. System designers often favor loose coupling between components, as it allows one component of the system to be changed without adversely affecting other components. One can think of a modern desktop computer as a loosely coupled system - for example, it is possible to remove a device (e.g. the CD drive) without being concerned that other parts of the system (monitor, keyboard etc.) will cease to function. At a lower level, each of these components is self-contained or encapsulated and integrates in the rest of the system via data channels (buses). It is this encapsulation that

poses constraints to only the individual component's design while allowing high level flexibility: changing the motor of a floppy disc or CD drive will likely require other changes in the device itself but will not affect the system design as a whole. This makes it easy for components to be added and removed while preserving the overall design blueprint of the system.

We see a very similar picture in genetic interactions networks: low-level functional modules are very highly conserved (immutable) with significant constraints over connections between modules involved in the same task (process). This allows for very economical design of different networks re-using the same small set of building blocks. Lesser restrictions are apparent over the wiring between different processes making this design paradigm very flexible and easy to evolve. And finally, similar to what is seen in computers, there appears to be a high level conservation of the flow of information through the network since the arrangement and thickness of GI bundles connecting different processes appears to be very similar between the two organisms.

Therefore, our data suggests that information collected from model systems about connections between individual genes would not be as useful as inferences derived from functional module definitions and cross-talk between different processes. However, it appears that general systems-level properties of the networks studied may be conserved across species. The knowledge that in two distantly related organisms certain categories of genes are genetic interaction hubs, and that certain pairs of processes are densely connected by genetic interactions, should facilitate the development of rational experimental designs to tackle the difficult problem of searching for epistasis in mammalian systems.

Methods

E-MAP data collection

Strain construction

Gene deletions were performed by homologous recombination of a linear DNA fragments carrying an antibiotic resistance marker (NAT or G418) flanked by long (> 200 bp) stretches of homology to the targeted region. For mutants available in the deletion library (Bioneer) query strains were constructed by marker switching (G418 to NAT resistance) and subsequent deletion construct amplification and transformation in the acceptor genetic background.

Raw data collection

Genetic crosses were performed in high density (1536 format) on a Singer RoToR station using the PEM system (Roguev et al., 2007) and applying a previously published protocol (Collins et al., 2010). NAT-marked query mutant strains with PEM2 genetic background (for full list, see Table S1) were crossed to a library (Bioneer) of G418-marked gene deletions for full list and library layout see Table S2 and double mutant phenotypes were scored using colony size as a readout. Data was collected in batches of 25-35 queries and digital images were obtained at 24 and 48 hours after the final plating step. Colony sizes were measured using the ColonyMeasure Program (<http://sourceforge.net/projects/ht-col-measurer/>).

Scoring of genetic interactions

Raw data was scored using a published MATLAB-based software toolbox (Collins et al., 2010). Individual batches were normalized and scored separately before merging into the final dataset, thus minimizing systematic experimental biases and batch-to-batch variation. Wrong strains (e.g. strains with mis-annotated genotype) were identified and removed by comparing the expected and observed linkage curves. The dataset was further pruned for mutants with very noisy profiles and/or poor reproducibility between replicate screens. Data points caused by genetic linkage were removed from each profile using an adaptive threshold procedure. Finally, the internal consistency of the data was tested by comparing pair-wise genetic interaction scores from marked-swap and replicate experiments.

Chapter 3: Chemical-Genetics of Rapamycin Insensitive TORC2 in *S. cerevisiae*

Introduction

Kinase signaling networks are primary regulators of cell growth and division. Improper signaling caused by mutations to kinases is a major driver of cancer progression (Greenman et al., 2007; The Cancer Genome Atlas Research Network et al., 2013; Wood et al., 2007). The success of targeting single kinases has been mixed due to rapidly emerging drug resistance and significant toxicity that limits the use of several of these agents to doses that do not block cancer growth (Boss et al., 2009; Haura et al., 2010). In contrast, the vast majority of clinically available therapeutics have multiple targets (Knight et al., 2010; Mestres et al., 2009). Many of these off-targets contribute to the therapeutic efficacy but also increase the toxicity and side effects of these drugs. Many preclinical and clinical studies have empirically searched for synergistic activities of kinase-targeted therapies but systematic studies are far less common. In this study, we endeavor to systematically study synergistic interactions with TOR kinase activity.

TOR is a primary integrator of proliferative signals and aberrant signaling by this kinase contributes to cancer (Casadio et al., 1999; Inoki et al., 2005; Kaeberlein et al., 2005; Martin and Hall, 2005; Tee and Blenis, 2005; Tischmeyer et al., 2003). As clinical use of selective inhibitors of TOR complex 1 (TORC1) (rapamycin and its derivatives, rapalogs) become more widespread in cancer treatment and ATP-competitive inhibitors of both TORC1 and TORC2 (including BEZ235, INK-128/MLN0128, KU-0063794, and WYE-354) reach the clinic, the search for secondary targets to use in combination therapy will gain urgency.

In addition to the clinical utility of an efficient method to find secondary targets to use in combination with TOR inhibitors, we were motivated by the fundamental lack of understanding of TORC2 biology resulting from the lack of pharmacology to selectively inhibit this complex. While prior studies have identified roles for TORC2 in cytoskeletal reorganization, sphingolipid biosynthesis and ribosome biogenesis (Beeler et al., 1998; Breslow et al., 2008; Helliwell et al., 1998b; Roelants et al., 2004; Schmidt et al., 1997; Zinzalla et al., 2011), it has been impossible to monitor these interactions on a rapid timescale made possible by pharmacological inhibition. It has also been impossible to specifically trace the function of these interactions to the ‘kinase activity’ of TOR.

While selective pharmacological inhibition of TORC2 in mammals is not easily achieved since both complexes share the same kinase, *S. cerevisiae* has two distinct kinase genes, TOR1 and TOR2 that can be independently inhibited. TORC1 can contain TOR1 or TOR2 and is rapamycin sensitive. TORC2 only contains TOR2 and is rapamycin insensitive (Loewith et al., 2002). The presence of distinct TOR kinases in yeast is a key advantage that enables independent modification of the active site of TOR2 using chemical genetics to generate a selective inhibitor for a modified allele of TORC2 (Bishop et al., 2000).

To study the selective pharmacology of TORC2 inhibition, we engineered an allele of TOR2 (as-TOR2) to accept an orthogonal kinase inhibitor that would not inhibit TORC1. To generate an unbiased map of the signaling network that TORC2 participates in and to furnish a list of interesting secondary targets for combination therapy, we determined chemical-genetic interactions between the TORC2 kinase and 1000 non-essential genes in *S. cerevisiae*. For comparison, we generated a chemical genetic

interaction dataset using the TORC1 inhibitor rapamycin. This approach enabled independent investigation of genetic interactions arising from the catalytic activity of either TOR complex.

Typically, genetic interactions report on how the function of one gene depends on the function of another. Negative interactions occur when two mutations cause the resulting double mutant to grow worse than expected relative to the growth rate of the two single mutants and indicates the two genes function in redundant or compensatory pathways. Positive interactions occur when the double mutant grows better than expected based on the phenotypes of the two single mutants suggesting the two genes function in the same complex or in a linear pathway (Beltrao et al., 2010; Collins et al., 2007; Fiedler et al., 2009; Kelley and Ideker, 2005; Roguev et al., 2008; Ryan et al., 2012; Schuldiner et al., 2005; Tong et al., 2004). Retaining this framework for interpretation, we developed a new tool for analysis of the dose-dependent effect due to drug treatment, termed Chemical Epistasis Mini-Array Profile (ChE-MAP).

ChE-MAP is a pharmacological extension of the powerful E-MAP technology that typically relies on the growth phenotype of double deletion mutants (Collins et al., 2006; 2010; Schuldiner et al., 2006) and enables dose-dependent kinase-gene interactions to be identified. The gene interactions are akin to an allelic series from hypomorphic (low dose drug treatment) to severe loss of function (high dose drug treatment). This approach contrasts with previous E-MAPs that used drugs to either induce or modify the phenotype in double-deletion mutants (Bandyopadhyay et al., 2010). Instead, interactions in our ChE-MAP result from the combined effects of a single deletion mutant and chemical

inhibition of TOR kinase activity. This analysis enables characterization of the TOR signaling network due to rapid inactivation of either TORC1 or TORC2.

We used the ChE-MAP approach to provide an unbiased view of interactions with the catalytic function of the two TOR complexes. The results recapitulate known regulatory relationships between TORC2 and sphingolipid biosynthesis. Statistical analysis revealed enrichment in metabolic processes and analysis of metabolic pathways revealed an interaction network signature suggesting involvement of TORC2 in regulation the pentose phosphate pathway (PPP). Further study showed levels of key metabolites in the PPP decreased in response to TORC2 inhibition, but not TORC1 inhibition, suggesting a specific and previously unappreciated role for TORC2 in regulating cellular ribosides.

Results and Discussion

A chemical-genetic tool for studying TORC2

Analog-sensitive kinases contain an active site mutation, termed the gatekeeper, that allows selective inhibition with a compound that is too bulky to fit into the active site of wild-type kinases (Bishop et al., 2000). This residue is typically a branched chain amino acid in the hydrophobic affinity pocket within the active site of the kinase (Buzko and Shokat, 2002). Mutation to a smaller residue permits binding of the bulky inhibitor.

Based on the homology of mTOR to PI3K γ , we performed a structure-based alignment to identify the gatekeeper residue (I2237) of *H. sapiens* mTOR (Figure 11A). Insertion of mTOR inhibitor BEZ235 into the active site guided by the affinity of backbone carbonyl of V2227 to the quinoline nitrogen (the most common mode of kinase inhibitor binding) shows a steric clash with the hydrophobic pocket that is exacerbated in

the presence of other branched chain aliphatic residues such as leucine (shown in grey). In contrast, the reported wildtype TOR inhibitor in yeast, QL-IX-55 (Liu et al., 2012), containing the 2-aminopyridine in place of the quinoline shows no steric clash. We reasoned that we could mutate the gatekeeper to a smaller residue in order to make space in the hydrophobic affinity pocket to accommodate a larger inhibitor. We then performed a sequence alignment to identify the conserved leucine gatekeeper in yeast TOR (Figure 11B). The gatekeeper residue of *S. cerevisiae* TOR2 was identified as L2178, mutated to alanine, and genomically integrated into the TOR2 locus yielding cells containing as-TOR2.

Since TOR2 kinase activity is essential in *S. cerevisiae*, replacement of TOR2 with a mutant that supports viability indicates that the as-TOR2 allele is catalytically active. Screening of the mutant kinase against a panel of ~40 ATP-analogs and kinase inhibitors (Appendix B, Figure S2) revealed that the as-TOR2 allele was selectively inhibited by a single agent, BEZ235, while the growth of wt-TOR2 was affected by this compound only at the highest concentrations tested (Figure 11B). Nearly equivalent growth rates of wild-type and analog-sensitive (as) alleles on YPD plates (Figure 11C) as well as in culture indicate the as-TOR2 is capable of supporting growth. Typical chemical scaffolds for inhibition of analog-sensitive kinases based on a pyrazolo-pyrimidine scaffold (Bishop et al., 2000), or compounds designed to target the gatekeeper residue of lipid kinases (Alaimo et al., 2005) showed no activity toward as-TOR2 (Appendix B, Figure S1). While BEZ235 is a potent mTOR inhibitor in mammals, it only has activity toward wild-type yeast at high concentrations (Figure 11C, 11D, 11E).

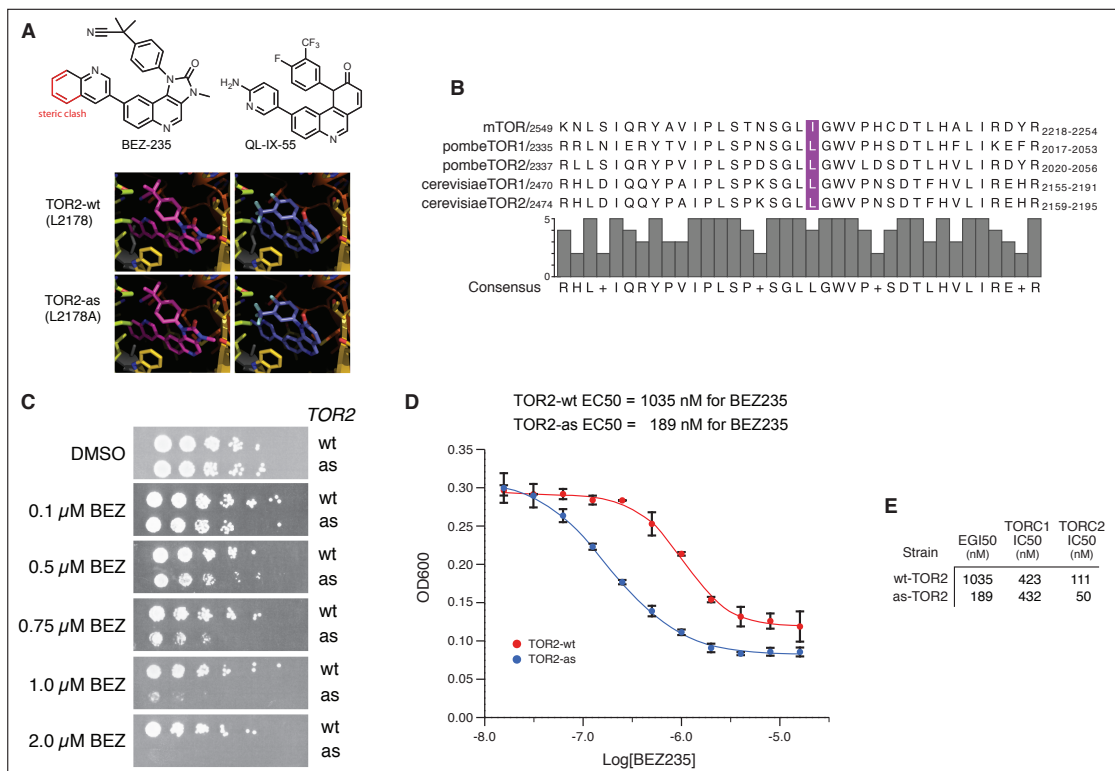


Figure 1

Figure 11. Modeling and Characterization of the as-TOR2 allele

(A) Homology model of mTOR based on the structure of PI3K γ shown with the gatekeeper residue in gray. The known *S. cerevisiae* TOR1/TOR2 inhibitor QL-IX-55 (purple) and BEZ235 (magenta) were oriented based on a typical h-bonding interaction with the backbone carbonyl of valine in the active site at VanDer Waals distances away from other residues that form the ATP-binding pocket. The isoleucine gatekeeper clash with BEZ235 is exacerbated by mutation to leucine and alleviated by mutation to alanine. The smaller QL-IX-55 does not sense this residue. (B) Sequence alignment shows the gatekeeper residue (in purple) is isoleucine in mTOR and leucine in all other cases. The active site is highly conserved. (C) as-TOR2 has an identical growth rate to wt-TOR2 when grown on YPD. At higher doses (1 μ M BEZ235), growth of as-TOR2 is inhibited while wt-TOR2 is unaffected. Growth of wt-TOR2 begins to be affected at 2 μ M BEZ235. (D) EC₅₀ of as-TOR2 and wt-TOR2 growing in culture. as-TOR2 is significantly more sensitive to BEZ235 than wt-TOR2. (E) IC₅₀ values show BEZ235 does not inhibit TORC1, that as-TOR2 does not play a significant role in the catalytic function of TORC1, and that the compound selectively inhibits as-TOR2 in TORC2 over wt-TOR2. The in vitro values correspond well to in vivo results which are typically less sensitive due to high concentrations of ATP and poor cell wall permeability of yeast.

To test that the analog-sensitive allele was selectively inhibited by BEZ235, we measured the cellular EC₅₀ of the as-TOR2 in liquid culture to be 189nM and wt-TOR2 to be 1035nM (Figure 11D). Since we planned to do the screen on agar plates, we also performed a dose series from 0.1-2.0 μ M BEZ235 (Figure 11C). Results show potent inhibition of the as-TOR2 strain and only a slight growth defect in wt-TOR2 cells at the highest concentration.

To determine whether this sensitivity was due to the TOR2 kinase, we performed in vitro kinase assays using TORC2 purified (with HA-tagged TSC11, a TORC2 specific component) from cells containing as-TOR2 or wt-TOR2. The kinase assay shows the IC₅₀ of BEZ235 for TORC2 is 50nM while the IC₅₀ for wild-type is 111nM (Figure 11E, Figure 12). The potency was measured at 100 μ M ATP. Since the mutation likely has the additional effect of increasing the K_m for ATP. The probable decrease in competition with ATP would further enhance the efficacy of BEZ235 in cells.

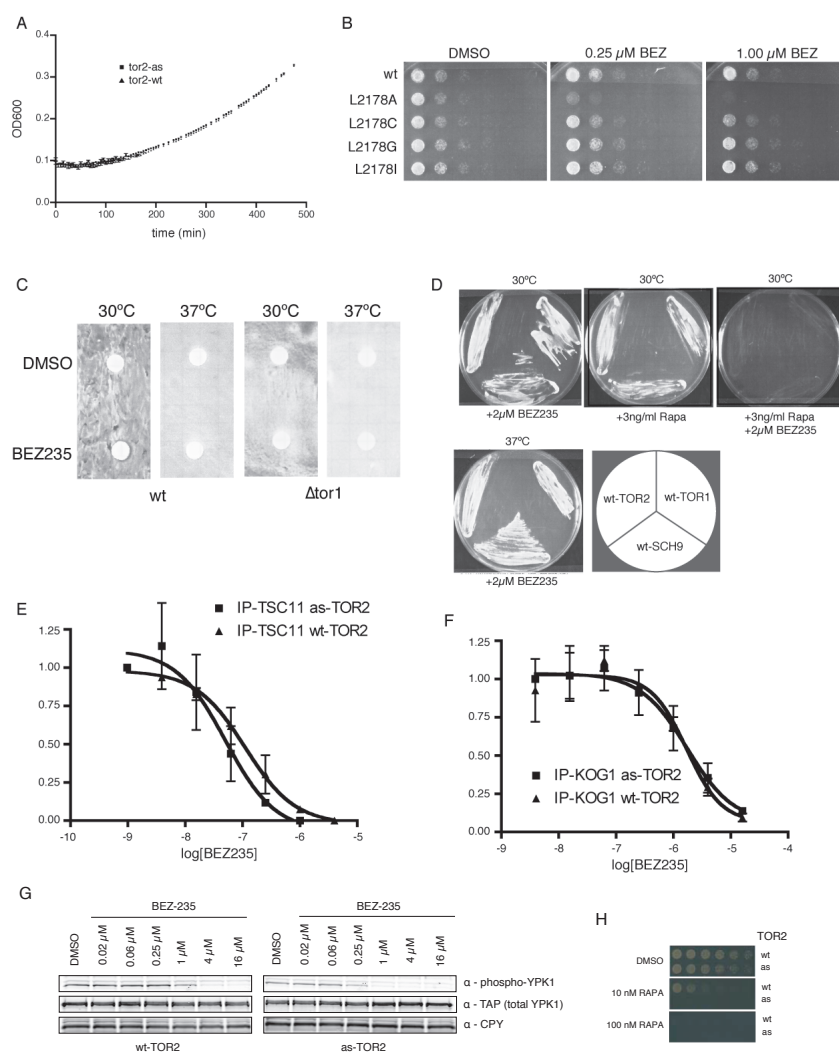


Figure 12. Characterization of the as-TOR2 mutant

(A) Growth of wt-TOR2 and as-TOR2 in YPD liquid cultures shown with standard deviations based on 3 measurements. (B) Growth of several TOR2 gatekeeper mutants on YPD with increasing concentrations of BEZ235 (C) Halo assay of BEZ235 in which VPS34 is perturbed at 37°C with Δ tor1 background. Lack of killing by BEZ235 indicates the compound does not hit VPS34 or TOR1. (D) Streak assay of wt-TOR1, wt-TOR2, wt-SCH9 with BEZ235 at 30°C and 37°C shows BEZ235 does not hit TOR1 or VPS34. Streak assay of wt-TOR1, wt-TOR2, and wt-SCH9 at 30°C with rapamycin and BEZ235 shows that marked alleles do not behave as DAMP strains (perturbed alleles). (E) IP-kinase assay shows in vitro IC_{50} of TORC2 is 50nM purified from as-TOR2 cells and to 11nM purified from wt-TOR2 cells. (F) IP-kinase assay shows in vitro IC_{50} of TORC1 is 432nM purified from as-TOR2 cells and 423nM purified from wt-TOR2 cells. (G) In vivo phosphorylation of YPK1 shows increased sensitivity of as-TOR2 to BEZ235 relative to wt-TOR2. (H) Spot test assay shows as-TOR2 is a perturbed allele since it is killed at a lower concentration of rapamycin than wt-TOR2.

Two potentially complicating factors in our analysis of TORC2 function through inhibition of as-TOR2 were first, the presence of TOR2 in TORC1 (Loewith et al., 2002) and second, the possibility that BEZ235 might simply inhibit TORC1 in the presence of a slightly weaker as-TOR2 allele. To test whether TOR2 was a major contributor to the activity of TORC1 and to see if BEZ235 inhibited TORC1, we purified TORC1 from as-TOR2 cells and wt-TOR2 cells. We found that inhibition of TORC1 by BEZ235 is approximately 4-fold less potent than wild-type TORC2 *in vitro*. The IC₅₀ of BEZ235 for TORC1 purified from wt cells is 423nM. This IC₅₀ is too weak to account for the potent growth inhibition of as-TOR2 since there is at least a 5-fold and sometimes a 100-fold shift in potency from *in vitro* IC₅₀ to *in vivo* EC₅₀ due to cellular competition with ATP and the poor permeability of the cell wall in yeast. This indicates BEZ235 does not inhibit TORC1, particularly at concentrations used in this study. Furthermore, the IC₅₀ of BEZ235 for TORC1 purified from as-TOR2 containing cells (432nM) indicates that there is not significant inhibition of any as-TOR2 that may participate in TORC1 (Figure 11E, Figure 12E, 12F).

To verify that as-TOR2 was selectively inhibited *in vivo*, we compared the phosphorylation of the well-characterized TORC2 substrate, YPK1, *in vivo*. While phospho-YPK1 does not show significant inhibition until 1 μ M BEZ235 in wild-type cells, it does show significant inhibition at 0.25 μ M in as-TOR2 cells (Figure 12G). Since phospho-YPK1 in as-TOR2 cells treated with DMSO is lower than wild-type overall, we can surmise the as-TOR2 allele is slightly perturbed. However, the results show that the kinase is functional and able to phosphorylate its substrates.

To further characterize the specificity of BEZ235 for as-TOR2, we investigated potential off target effects of the compound. We ruled out off-target effects of BEZ235 on essential kinases in the same family (MSS4 and PIK1) since these would have resulted in growth inhibition of wild-type cells. To test if BEZ235 was targeting PI3K ortholog VPS34, we made VPS34 conditionally essential in Δ TOR1 background and observed no growth inhibition by BEZ235 (Figure 12C). The compound also shows no activity toward wt-TOR1 or wt-TOR2 alleles when perturbed at high temperature or pharmacologically using rapamycin (Figure 12D).

To test if BEZ235 was a general chemical scaffold that could be used to selectively inhibit analog-sensitive alleles of other family members, we screened as-MEC1 (Alaimo et al., 2005) against a structurally diverse subset of compounds that were previously used to screen as-TOR2. None of the compounds except rapamycin had any activity toward wild-type cells. Only BEZ235 inhibited as-MEC1 and showed no activity toward wt-MEC1 strains (Appendix B, Figure S1). This suggests this compound may be a generalizable scaffold for inhibiting as-kinases in the PIKK family.

To characterize genetic interactions resulting from selective inhibition of TORC1, we performed screens with the wild-type allele in the presence of rapamycin and with the as-TOR2 allele in the presence of BEZ235. These datasets shed light on the distinct signaling networks of TORC1 and TORC2 and provides the first unbiased *and* selective investigation of genetic interactions with TORC2 kinase activity (Figure 13A).

A global map of genetic interactions with the TOR2 kinase

To systematically investigate synergistic interactions with TORC2, we combined our chemical-genetic tool with high-throughput yeast genetics to quantitatively assess the

strength of synergistic interactions against a broad set of deleted genes. We systematically crossed either wt-TOR2 or the as-TOR2 allele with a library of ~1000 non-essential deletion mutants and selected for the haploid double mutant strains (Figure 13B). By growing strains on synthetic complete media containing either DMSO or increasing concentrations of rapamycin or BEZ235, we were able to measure dose-dependent growth phenotypes of mutant yeast colonies and use these phenotypes to compute individual genetic interaction scores. These screens were done in the presence of several other unrelated queries (Appendix B, Table S4) to ensure robust statistics required for accurate calculation of S-scores (Collins et al., 2006; 2010; Schuldiner et al., 2006).

To evaluate the strength of the chemical-genetic interaction with either TOR complex, we computed S-scores for all observed strains. An S-score is a quantitative assessment of the strength and reproducibility of the interaction between two alleles (Collins et al., 2006; 2010). For interactions that showed a consistent *and* directional trend in correlating with drug dose, we calculated a difference score ΔS ($\Delta S = \text{High Drug} - \text{DMSO}$). Since ΔS is a close analog to S-score, and $S = 2.6$ has been used previously as a cutoff for significance in published literature (Fiedler et al., 2009), we chose $\Delta S \geq |2.6|$ as a cutoff for significance in our analysis.

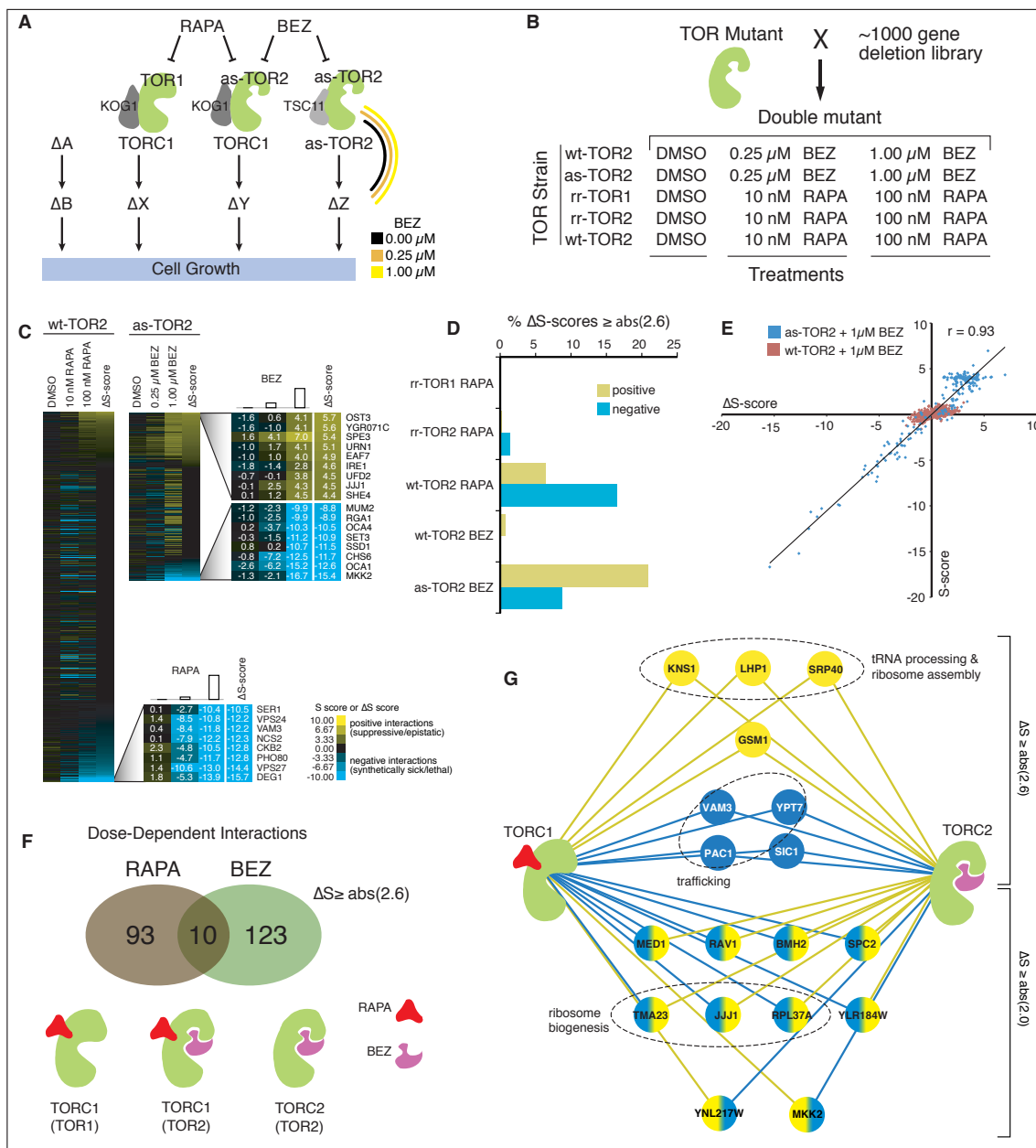


Figure 2

Figure 13. Chemical Epistasis Mapping of TORC1 and TORC2

(A) TOR1 exists only as a member of TORC1. TOR2 may exist as a member of either TORC1 or TORC2. Rapamycin selectively inhibits TORC1. BEZ235 is selective for the as-TOR2 allele. Chemical-genetic interactions behave as traditional double deletion mutants. For interacting genes, a directional shift between the DMSO control and the [high] drug screen should occur. Dose-dependent positive interactions occur between genes in linear pathways, dose-dependent negative interactions occur between genes in parallel pathways. (B) TOR mutant strains were mated to a library of ~1000 non-essential single deletion mutants. The resulting double mutants were grown on plates containing DMSO or increasing concentrations of rapamycin or BEZ235.

(C) ChE-MAP for rapamycin treated and BEZ235 treated datasets sorted according to ΔS -score. The strength of positive and negative chemical-genetic interactions (S-scores) are reported by yellow or blue squares respectively. Inset are top hits from each set. The as-TOR2 dataset is significantly smaller since many strains were very sick at the highest concentration of BEZ235 and were removed during quality filtering. (D) Experimental datasets (wt-TOR2+rapa, as-TOR2+BEZ) and control datasets (rr-TOR1+rapa, rr-TOR2+rapa, wt-TOR2+BEZ) are shown by percent of total interactions in the dataset above $\Delta S \geq |2.6|$. Positive interactions are in yellow, negative interactions are blue. Rapamycin and BEZ235 are selective for their intended targets and generate few off target interactions. (E) Scatterplot of ΔS -score vs S-score illustrates the specific effect of BEZ235 on as-TOR2. wt-TOR2 (red) is unaffected by the compound and cluster around 0. as-TOR2 (blue) is strongly affected and shows a direct relationship between ΔS -score and S-score at $1\mu\text{M}$ BEZ235. (F) Number of dose-dependent genetic interactions above a $\Delta S \geq |2.6|$ in each set. 104 interactions recorded for rapamycin, 134 recorded for BEZ with overlap of 10. (G) Network illustrating genes that hit both TORC1 and as-TOR2 above specified threshold. Nodes and edges are colored yellow for positive or blue for negative interactions with the indicated complex.

Three of these datasets are experimental controls for off-target effects of the compounds (Figure S4). wt-TOR2 cells were treated with the same concentrations of BEZ235 as as-TOR2, and rapamycin resistant (rr) alleles (Cafferkey et al., 1993; Heitman et al., 1991; Helliwell et al., 1994) of TOR1 and of TOR2 (S1972I-TOR1 and S1975I-TOR2) were treated with rapamycin. The limited number of genes that showed dose-dependent interactions with the drug-resistant alleles were filtered from the experimental datasets. The two experimental datasets reveal dose-dependent genetic interactions between specific yeast genes and rapamycin or BEZ235 (Figure 13A; Appendix B, Table S1). The examined library of yeast genes includes genes from all functional categories, including regulatory proteins, signaling machinery, cell cycle regulators, and metabolic enzymes (Appendix B, Table S2).

Characteristic dose dependent ChE-MAP interactions

Analysis of ChE-MAPs generated with wild-type cells mated to deletion mutants and grown on 0, 0.25 μ M, and 1 μ M of BEZ235 show the compound is selective for the analog-sensitive allele with few off-target effects (Figure 13D). Only three dose-dependent genetic interactions are seen above $|\Delta S| \geq 2.6$ in the wild-type dataset suggesting that our method identifies few false positives. We analyzed the distribution of S-scores for wt-TOR2 and as-TOR2 at 1 μ M BEZ235 (Figure 13C). Based on previous E-MAP datasets, our expectation was that wt-TOR2 would show characteristic single mutant phenotypes with S-scores at or near zero. This phenotype should persist at all drug doses if BEZ235 is selective for as-TOR2. At the highest dose of BEZ235, we observe a clear direct relationship between S-score and ΔS in cells containing as-TOR2. In contrast, there is no relationship between S-score and ΔS when 1 μ M BEZ235 is

applied to the wt-TOR2 cross. While the S-score is a useful reference for quantification, it does not account for allelic effects of our point-mutants or genetic markers, which are not always silent in genetic analysis. By relying on ΔS , we are able to filter out allelic interactions that show strong phenotypes on DMSO and consequently do not fall along the diagonal in Figure 13C.

Drug resistant alleles showed very few dose-dependent interactions and the interactions observed were most likely due to allelic effects from the resistance marker. The rr-TOR1 showed no dose-dependent genetic interactions upon drug treatment. With the rr-TOR2 allele, 7 genes showed chemical-genetic interactions above threshold (*YPL150W*, *CKA2*, *BRE1*, *YPT7*, *IPK1*, *OPI11*, *THP3*). Dose-dependent interactions with the rr-TOR2 allele can arise from wt-TOR1 in TORC1, which can be inhibited by rapamycin in the rr-TOR2 strain background. These results are consistent with the fact that TOR1 is the primary kinase responsible for the outputs of TORC1 and supports our contention that rapamycin is highly specific for the complex.

Two hundred twenty-six dose-dependent ChE-MAP interactions were identified for rapamycin and BEZ235 at our cutoff of $\Delta S \geq |2.6|$. We observed 103 rapamycin-specific dose-dependent interactions and 123 BEZ235/as-TOR2-specific interactions with an overlap of 10 genes that show a dose-dependent effect with both (Figure 13D). Eight of these shared interactions show a dose-dependent effect that is the same whether TORC1 or as-TOR2 is inhibited (Figure 13E). We infer the positive interactions that arise are due either to a shared function of both complexes or to TOR2 participating in TORC1. The four negative interactions are compensatory with both TOR2 and TORC1.

Two genes (*RAV1*, *TMA23*) show positive interactions $\Delta S > 2.6$ with as-TOR2 and negative interactions $\Delta S < -2.6$ with TORC1.

Relaxing our cutoff to $\Delta S \geq |2.0|$, eight additional dose-dependent interactions were identified common to both the rapamycin and BEZ235 datasets (Fig. 13E; Appendix B, Figure S3). Six genes (*MED1*, *BMH2*, *RPL37A*, *JJJ1*, *SPC2*, *YLR184W*) show positive interactions with TORC2 and negative interactions with TORC1. Two genes (*MKK2* and *YNL217W*) are negative with TORC2 and positive with TORC1. The network view provides a full account of dose-dependent interactions observed with each TOR complex.

Several genes that interact with both TORC1 and TORC2 play important roles in ribosomal maturation. Our results show strong positive interactions with *KNS1*, *LHP1* and *SRP40* all of which participate in tRNA processing and ribosome maturation (Figure 13E) suggesting an important role for both TORC1 and TOR2 in these processes. While the role of TORC1 in phosphorylation of ribosomal protein S6 (RPS6) via S6-kinase (S6K) is known (Chung et al., 1992; Feldman et al., 2009; Price et al., 1992; Richardson et al., 2004; Urban et al., 2007), the involvement of TORC2 was not appreciated until recently (Zinzalla et al., 2011). Our data supports a role of TORC2 in ribosome biogenesis since two genes (*TMA23*, *JJJ1*) involved in ribosome biogenesis (Fleischer et al., 2006; Meyer et al., 2007) and a ribosomal protein (*RPL37A*) show strong positive interactions with TORC2 while simultaneously showing strong negative interactions with TORC1 (Figure 13E) indicating these genes are in a pathway with TORC2 and offering additional evidence that ribosomal biogenesis plays a role in regulating TORC2 (Zinzalla et al., 2011).

Enrichment of Sphingolipid Biosynthesis in TORC2 ChE-MAP hits

Next we looked in our datasets for well-characterized signaling pathways downstream of TORC2. Specifically, the sphingolipid biosynthesis pathway is the best characterized pathway under the control of TORC2 (Aronova et al., 2008; Beeler et al., 1998; Tabuchi et al., 2006). TORC2 is known to directly phosphorylate and regulate Ypk1/2 (Aronova et al., 2008; Kamada et al., 2005; Niles et al., 2012) and Ypk1/2 in turn phosphorylates and inactivates Orm1 and Orm2, which negatively regulate sphingolipid biosynthesis in the unphosphorylated state (Breslow et al., 2010; Niles et al., 2012; Roelants et al., 2011; Sun et al., 2012). We found extensive evidence for sphingolipid biosynthesis positively interacting with the kinase activity of TORC2 (Figure 14A).

The dose-dependent chemical genetic interactions between TORC2 and sphingolipid biosynthesis serve as a biological benchmark for the technique. We observe strong dose dependent chemical genetic interactions between TORC2 and *ORM2* (+3.4), *DPL1* (+3.9), *LCB4* (+4.2), and *ISC1* (+4.4), all of which play integral roles in the pathway (Figure 14A). No interaction is observed with TORC1, in good agreement with prior findings.

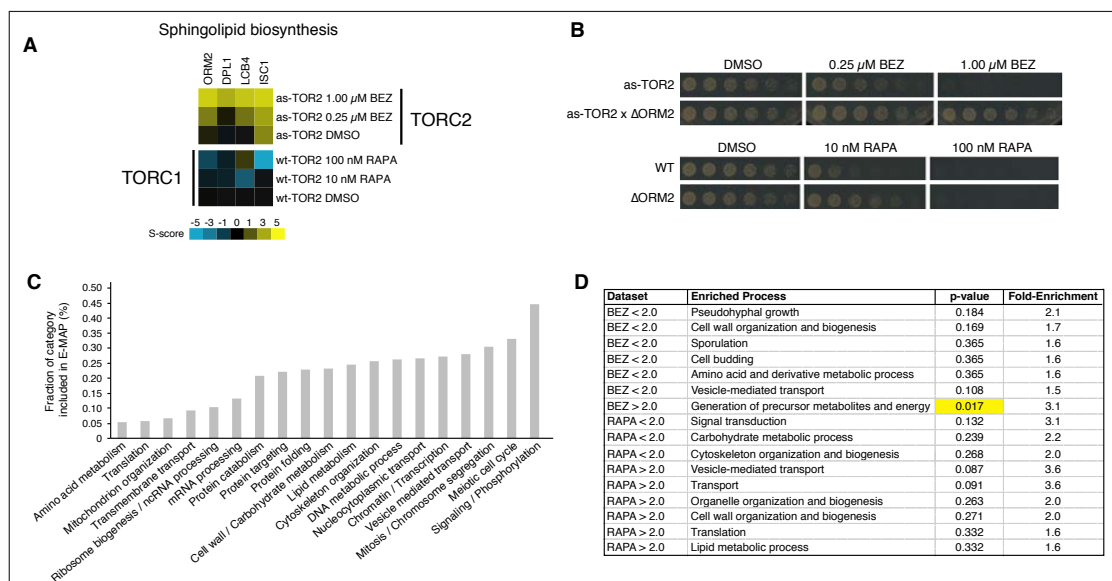


Figure 3

Figure 14. Enrichment in Biological Processes

(A) Bar graph shows fraction of each functional biological category that was included in the E-MAP. (B) Enrichment in either of the two datasets above or below $\Delta S = 2.0$ were calculated using a Fisher's exact test to identify terms in the cellular process GO Slim that were significantly enriched. Significant p-values are highlighted in yellow. (C) The sphingolipid biosynthesis pathway shows consistent dose-dependent behavior across all members of the pathway that were included in the screen in good agreement with theoretical prediction. S-score is indicated on a color metric scale with blue as strongly negative and yellow as a strong positive interaction. (D) Genotyped and sequenced members of pulled tetrads grown on plates containing increasing concentrations of rapamycin or BEZ235 confirm phenotypes tested using the ChE-MAP.

To confirm this phenotype, we performed tetrad analysis with these mutants and subjected the appropriate crosses matching the ChE-MAP results to increasing concentrations of rapamycin and BEZ in a spot dilution assay (Figure 14B). The results show that Orm2 shows a positive phenotype upon as-TOR2 inhibition. The positive genetic interactions with several members of the sphingolipid biosynthesis pathway validate the ChE-MAP as a viable strategy for identification of downstream signaling pathways.

Cellular Compartment and Process Enrichment of TORC2 Interactions

Using the ChE-MAP interaction data, we asked whether there was functional enrichment for genes annotated in a particular cellular compartment or biological process. Our results were not biased since we included a diverse and balanced collection of queries in the ChE-MAP (Figure 14C).

TORC2 interacting genes were analyzed for gene ontology (GO) terms for cellular compartment showed a two-fold enrichment for proteins that localize to the endoplasmic reticulum ($p < 0.05$), controlling for sampling bias in the gene deletion library used for this study. This result is consistent with recent work showing mammalian TORC2 co-fractionates with the ER (Boulbés et al., 2011), suggesting the localization of TORC2 is conserved and expands our understanding of previous work showing TORC2 in *S. cerevisiae* localizes to the plasma membrane and regulates sphingolipid biosynthesis (Berchtold and Walther, 2009; Berchtold et al., 2012). TORC1, by contrast, localizes in the vacuole of *S. cerevisiae* and to the lysosome surface in mammalian cells (Berchtold and Walther, 2009; Loewith et al., 2002; Zoncu et al., 2011).

Next, we analyzed the TORC1 and TORC2 datasets for enrichment of hits mapping to specific biological processes. While no significant enrichment was observed with hits greater than $\text{abs}(2.0)$ or less than 2.0 , enrichment was observed for positive hits (genes predicted to be in pathway with TORC1 or TORC2). Although not significant ($p = 8.7 \times 10^{-2}$), the enrichment of TORC1 hits for ‘vesicle-mediated transport’ is consistent with published reports that show rapamycin treatment decreases phosphorylation of proteins involved in vesicle mediated transport ($p = 6.0 \times 10^{-4}$) (Yu et al., 2011).

While TOR has been loosely associated with energy homeostasis for many years due to the obvious energetic demands of protein synthesis and ribosome biogenesis, a link with metabolite synthesis was not previously shown. Our ChE-MAP revealed significant enrichment ($p < 0.05$) for ‘generation of precursor metabolites and energy’ for positively interacting TORC2 hits (Figure 14D). To investigate this further, we sought to integrate published physical interaction data with our chemical genetic results to see if there were specific metabolic processes with predominantly positive interactions with TORC2.

Integrated functional network of TOR signaling

To look for proteins involved in metabolite synthesis that physically interact with TOR, we searched for genes in metabolic GO terms that had large numbers literature reported (Stark et al., 2006) physical interactions with members of the TOR signaling pathway. We found that many proteins in the pentose phosphate pathway (PPP) have physical interactions with proteins in the TOR signaling pathway compelling us to construct a comprehensive network of PPP proteins that physically interact with each of the TOR complexes.

The network of genes that are annotated (by GO terms) to the PPP shows a distinct signature with TORC1 genes compared with TORC2 genes (Figure 18a). The figure shows that many enzymes that catalyze steps in the PPP physically interact with proteins that positively interact with as-TOR2 (*BDF2*, *GAC1*, *URN1*, *YPL150W*). In contrast, enzymes in the PPP generally show physical interactions with proteins that negatively interact with TORC1 (*TPM1*, *SET2*, *HAT2*). The network shows exclusively positive interactions with TORC2 and predominantly negative interactions with TORC1, suggesting the PPP is in a linear pathway with TORC2, and a parallel pathway to TORC1. This phenotype is the hallmark of a TORC2 regulated pathway and motivated us to investigate whether metabolite levels and particularly the PPP was regulated by TORC2.

Metabolomic analysis of TORC1 and as-TOR2

To test the role of TORC2 in the PPP, we used reverse-phase ion-paired LC/MS to monitor drug dependent changes to over ~130 cellular metabolites including constituents of the PPP pathway (Figure S5). Rapid metabolic changes that take place soon after drug treatment suggest direct regulation of metabolic enzymes while changes that occur on the timescale of yeast cell replication/division are more likely to indicate transcriptional changes to metabolic enzymes.

As an internal quantitative and qualitative reference for the magnitude of the metabolic changes and a point of comparison for our drug treatment, we also assessed metabolic changes due to nitrogen starvation. Nitrogen-starvation is akin to rapamycin in that it disrupts phosphorylation of TORC1 substrates (Urban et al., 2007). To identify changes to metabolite levels in response to inhibition of TOR components, cells were

treated with inhibitors or switched to low-nitrogen media and metabolic changes were quantified over time by LC/MS to look for inhibitor dependent changes in soluble metabolite levels.

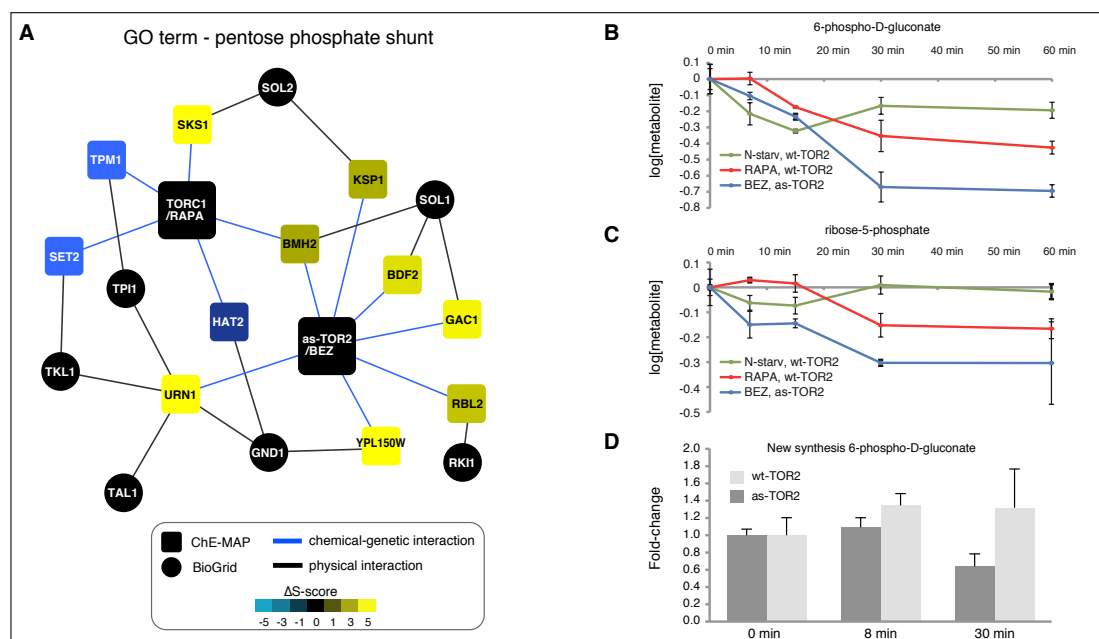


Figure 4

Figure 15. Effect of rapamycin and BEZ235 on metabolites in the PPP

(A) Network of ChE-MAP hits that have physical interactions with genes within the PPP gene ontology term. Rounded rectangles and blue edges indicate chemical-genetic interactions and are colored according to the ΔS -score for the indicated gene. Black nodes indicate genes not found in our dataset (www.thebiogrid.org) or in the following citations: (Fan et al., 2008; Fasolo et al., 2011; Graille et al., 2005; Hesselberth et al., 2006; Krogan et al., 2006; Ptacek et al., 2005; Yu et al., 2008). Black edges indicate a physical interaction. (B) 6-phospho-D-gluconate levels quantified by LC/MS over a 60 minute time-course where cells are perturbed by nitrogen starvation, inhibited with rapamycin (wild-type), or inhibited with BEZ235 (as-TOR2). (C) Ribose-5-phosphate levels quantified by LC/MS over a 60 minute time-course where cells are perturbed by nitrogen starvation, inhibited with rapamycin (wild-type), or inhibited with BEZ235 (as-TOR2). (D) Isotope labeled 6-phospho-D-gluconate allows direct measurement of newly synthesized metabolite in as-TOR2 and wt-TOR2 cells and allows quantification of oxidative pentose phosphate pathway flux. Treatment with BEZ235 shows a significant change (**) after the short 30 minute timepoint.

Inhibition of TORC1 or as-TOR2 leads to broad changes across all aspects of metabolism. It is clear from the results that some changes result from the introduction of the as-allele alone since several of the metabolites measured show some change at time zero of the experiment. To correct for this, we filtered the metabolic results to capture the change in response upon drug inhibition over the 60 minute time-course [$\Delta M = \log(\text{as-TOR2/wt-TOR2})_{t=0\text{min}} - \log(\text{as-TOR2/wt-TOR2})_{t=60\text{min}}$]. After 1 hour of drug treatment, above a threshold of $\log(\text{metabolite}) \geq |1.5|$, nitrogen-starvation shows changes in 18 metabolites out of 123 measured, rapamycin shows changes in 23 metabolites out of 123 measured, while BEZ235/ as-TOR2 treatment affects 56 out of 120 metabolites measured. Inhibition of TOR2 affects more metabolites suggesting that TORC2 has a greater regulatory role in metabolism than TORC1.

We observed that metabolic intermediates involved in the PPP are strongly downregulated in response to as-TOR2 inhibition. In our experiments 6-phospho-D-gluconate (6PG) and ribose-5-phosphate (R5P), two intermediates that are specific to the PPP, show a rapid time-dependent response to treatment with BEZ235 (Figure 15B, 15C). R5P is the product of the oxidative pentose phosphate pathway and was recently shown to be produced by riboneogenesis (Clasquin et al., 2011). While this metabolite is perturbed due to the as-TOR2 allele, the metabolite shows an additional time-dependent decrease in levels after 7 minutes of treatment with BEZ235. These changes may suggest a role for TORC2 in regulating both the oxidative and non-oxidative branches of the PPP.

In contrast, the delayed down-regulation in response to TORC1 inhibition is consistent with previously proposed models that put enzymes in the PPP under the

control of transcription factors downstream of TORC1 (Düvel et al., 2010; Robitaille et al., 2013). The rapid response upon BEZ235 treatment indicates that TORC2 may have more direct control over the PPP through kinase signaling. This hypothesis is supported by GO analysis of the ChE-MAP (Figure 15A) that shows seven proteins with chemical-genetic interactions with TORC2 are also annotated to physically interact with metabolic enzymes of the PPP. All of these are positive interactions indicating they are in a linear pathway with TORC2. Strong positive interactors with TORC2 include *BDF2* and *GAC1*, which both physically interact with tRNA export protein Sol1, a close homolog of Sol3/Sol4 that catalyze the second step of the PPP leading to the generation of 6PG. Strong interactions are also observed between TORC2 and *RBL2* which physically interacts with Rki1. Rki1 regulates the third step in the PPP leading to the production R5P.

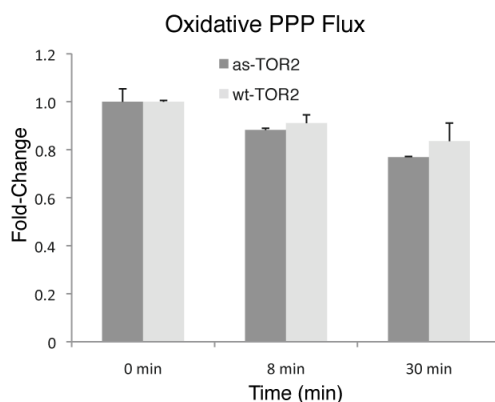


Figure 16. Flux through the oxidative PPP

Flux through the oxidative PPP does not change with BEZ235 treatment in as-TOR2 cells

To test whether TORC2 was influencing metabolite levels in the PPP by direct regulation of metabolic flux, we undertook analysis of using the tracer 1,2-¹³C-glucose to quantify levels of 6PG and R5P and to measure the relative ratio of oxidative PPP and

non-oxidative PPP transketolase reaction. The rapid decrease of 6PG in the as-TOR2 strain upon BEZ235 addition (Figure 15D) confirms TORC2's posttranslational regulation of the oxidative PPP since the change in metabolite levels occurs on a rapid timescale (< 30 minutes) as previously observed. The lack of substantial change of oxidative PPP flux (Figure 16) in the as-TOR2 strain relative to wild-type upon BEZ235 treatment suggests TORC2 does not differentially regulate the oxidative and non-oxidative PPP, and may regulate the PPP upstream of the split between the oxPPP and non-oxPPP, likely through differential regulation of glucose-6-phosphate dehydrogenase (the reaction upstream of 6-phosphogluconate) and 6-phosphogluconate dehydrogenase.

Conclusions

Yeast screens remain the most versatile tool for assessing functional genomic interactions at the organismal level. Genetic knockouts are facile for non-essential genes, but other methods are required for queries of essential genes such as the TOR2 kinase. Among these, decreased abundance by mRNA perturbation (DAmP), temperature-sensitive degrons designed to rapidly degrade proteins at the restrictive temperature, or chemical inhibitors for a specific target are the most commonly employed techniques. Use of DAmP alleles can be unreliable due to variable levels of knockdown. Temperature-sensitive (ts) strategies are effective but can suffer from pleiotropy. In particular, several different TOR2-ts isolates have been reported to have widely varying effects on cell cycle, budding, and actin structures at the restrictive temperature (Helliwell et al., 1998a). Chemical inhibitors are fast-acting, but the number of interesting essential targets far exceeds existing chemical tools to inhibit them.

In this study, we created a chemical-genetic tool that is highly specific and allows rapid inactivation of the TOR2 kinase. We used this tool to systematically and quantitatively probe the genetic interaction landscape of TORC2 kinase activity *in vivo*. We confirmed the robustness of our technique through its positive identification of sphingolipid biosynthesis downstream of TORC2 and show a significant enrichment in functional connections with proteins localized to the endoplasmic reticulum. Chemical-genetic interaction data show enrichment for ‘generation of metabolites and energy’ which directed us to investigate the PPP with physical interaction networks that showed a pattern of interactions that is consistent with the PPP existing in a linear pathway with TORC2. By performing by studying metabolite levels with as-TOR2 in the presence of BEZ, we were able to observe large and rapid (< 30 min) changes in metabolites that are created in the PPP and further showed these changes necessarily occur upstream of the transketolase reaction since data does not suggest a differential flux through the non-oxidative and oxidative PPP. This indicates that TORC2 may have a role in post-translational (by phosphorylation rather than transcriptional or translational) regulation of nucleotides required for protein synthesis.

The suggestion of a role for TORC2 in ribosomal biogenesis has interesting implications for how the cell balances energy demands to meet these needs. Emerging evidence indicates TORC2 is an important node in ribosome biogenesis (Zinzalla et al., 2011). The high energy requirements of ribosome biogenesis creates high demand for ribose relative to NADPH leading to activation of the PPP and production of R5P (Clasquin et al., 2011). Our evidence shows that TORC2 positively regulates metabolite synthesis in the PPP (Figure 15D), and may act as a critical relay between ribosome

biogenesis and the PPP. This is particularly compelling in conjunction with evidence showing that upregulation of the non-oxidative PPP is required for tumor survival (Deberardinis et al., 2008).

Our approach represents a unique union of genetics and pharmacology that facilitates rapid assessment of gene selective effects that could act as a first line of evidence in the search for synergistic therapeutics. It allows for a more granular analysis of functional genetic interactions that refer specifically to the catalytic activity of the kinase rather than scaffolding roles that the Tor protein certainly plays. These findings will be valuable for deciphering the different physiological roles of TORC1 and TORC2 in yeast. Such understanding in turn may help understand the roles of these complexes in mammals, where this approach cannot be directly applied, and thereby aid in the design of combination therapy regimens involving TOR inhibitors.

Experimental Procedures

Generation of point mutants

The C-terminal region TOR1 or TOR2 (including the FAT, FRB, kinase domain, and 160 bp of 3'UTR) was cloned onto plasmid pFA6-NAT-MX6, into the multiple cloning site immediately preceding the NAT gene (which confers resistance to Nourseothricin, Werner Bioagents). as-TOR2 (L2178A), rr-TOR2 (S1975I), and rr-TOR1 (S1972I) mutants were generated using site directed mutagenesis. These mutants were amplified using PCR and transformed into the BY4742 strain, in which the C-terminal region of either TOR1 or TOR2 had been displaced by k.1 URA3. Following selection on NAT and 5-FOA, the mutants were sequenced to confirm insertion of the desired mutations. Subsequently, the diploid mutant strains were sporulated and the mat alpha

haploid strains were selected for as described previously, and presence of the mutation was again confirmed by sequencing.

E-MAP experiments

Strain construction, plating of mutants, mutant selection, and scoring of genetic interactions (S-scores) were performed as previously described (Collins et al., 2006; Schuldiner et al., 2005). Using a Singer Instruments pinning robot, haploid double mutants were simultaneously grown in 1536-well format at 30 degrees Celsius on agar plates containing DMSO or containing a selective TOR inhibitor. Mutants in this study were screened in tandem with a large number of queries to ensure robust statistics for averaging ($n > 30$). Several unrelated queries, strains containing point mutants to SCH9, wild-type strains containing a TOR1 marker, a ts-TOR2 allele were used as query strains. For the plates containing inhibitor, 0.25 μ M BEZ235, 1.00 μ M BEZ235, 10nM rapamycin, or 100nM rapamycin were added to the plates containing selective media. Plates were photographed and the area of each colony was converted into pixels to quantitatively assess colony size. In untreated or treated conditions, colony sizes were based on 3 replicate measurements. For a given double mutant, the experimental data was used to assign a quantitative S-score based on a modified T-test that compares the observed double mutant growth rate to an expected growth rate based on the average colony size across an entire plate.

Dose-dependent interaction scoring system

Dose-dependent genetic interactions were identified for a given gene by searching for a series of S-scores for that gene that show a directional shift that correlates with drug

concentration. The magnitude of the interaction was evaluated as the difference between the high-dose and the control strain ($\Delta S = S\text{-score}_{\text{highdrug}} - S\text{-score}_{\text{DMSO}}$). ΔS -scores $\geq |2.6|$.

Enrichment of TORC2 dose-dependent interactions

Genes with a dose-dependent interaction $\Delta S \geq |2.0|$ were tested for enrichment in a specific cellular compartment. A Fisher's exact test was used to identify terms in the cellular compartment GO Slim that were significantly enriched in dose-dependent hits, resulting in the observation that dose-dependent hits are ~ 1.6 times more likely to be localized to the endoplasmic reticulum than expected ($p < 0.05$ after correcting for multiple testing). The background for this calculation was all mutants with measured scores from the as-TOR2 + BEZ235 screen, and consequently the observed enrichment is not due to the bias on the array, or due to data quality filtering.

The same approach was used to identify terms in the Biological Process Ontology showing significant enrichment for dose-dependent. All process terms having 1.5-fold or better enrichment are shown in Figure 3.

Tetrad Analysis

wt-TOR2 and as-TOR2 were mated to a single delete (SD) strain of interest for 48 hours prior to sporulation at room temp for 3-5 days. Digested ascus with zymolyase for 20min prior to tetrad dissection. Replica plated tetrads on selective media for genotyping and verified all strains using check PCR and sequencing of the TOR kinase domain locus.

Spot Test Assay

Overnight cultures were grown to saturation, diluted to $OD_{600} = 0.2$ and grew until all four strains were $OD_{600} = 0.8$. 2-fold serial dilutions of cells were plated on DMSO,

0.1 μ M, 0.25 μ M, and 1 μ M BEZ235 or on 10nM 50nM, 100nM rapamycin. Plates were grown at 30°C and imaged after 24h.

Gene Ontology Network Analysis

Circular nodes were created for all genes within a given GO term. Then, rectangular nodes were generated for hits in either the rapamycin or BEZ235 datasets and were linked to the circular nodes based literature reported physical interactions (Stark et al., 2006). Genetic interactions between TORC1 or as-TOR2 computed and illustrated using blue edges.

Metabolite Measurement

The metabolome of *Saccharomyces cerevisiae* was characterized as described previously (Xu et al., 2012). Saturated overnight cultures were diluted 1:30 and grown in liquid media in a shaking flask to A600 of \sim 0.6. A portion of the cells (3 mL) were filtered onto a 50 mm nylon membrane filter, which was immediately transferred into – 20°C extraction solvent (40:40:20 acetonitrile/methanol/water). Serial extraction was then carried out at indicated time points after drug treatment. Cell extracts were analyzed by reversed phase ion-pairing liquid chromatography (LC) coupled by negative-mode electrospray ionization (ESI) to a high-resolution, high-accuracy mass spectrometer (Exactive; Thermo Fisher Scientific) operated in full scan mode at 1 s scan time, 10^5 resolution, with compound identities verified by exact mass and retention time match to authenticated standard (Rabinowitz et al., 2010). Isomers are reported separately only where they fully chromatographically resolved.

Metabolic Flux Measurement

Yeast cells were grown in 1,2-¹³C₂-glucose in the presence of 1 nM or 5 nM estradiol. The use of 1,2-¹³C-glucose allows measurement of oxidative pentose phosphate pathway flux. All the isotope-labeled forms of ribose phosphate are quantitated. The flux is calculated as following: Oxidative pentose phosphate pathway flux = $(f_1 + f_2)/(f_3 + f_4 - f_0)$ in which f_n is the labeling fraction of the n-labeled ribose phosphate. The oxidative branch of the pentose phosphate pathway yields 1- and 3-labeled pentose phosphate. The non-oxidative branch of the pentose phosphate pathway yields 2- and 4-labeled pentose phosphate. One molecule of 0-labeled pentose phosphate is generated for every 2- or 4-labeled pentose phosphate produced through erythrose phosphate. Therefore 0-labeled pentose phosphate is subtracted to reflect the true flux of non-oxidative pentose phosphate pathway.

Appendix A: Chapter 2 Supplemental

Supplemental Tables

Available online (<http://www.cell.com/molecular-cell/>; Ryan et al. (2012) supplemental information)

Table S1. Gene Annotations

Table S2. Functional Module Definitions

Table S3. Between-Process Enrichments and P Values

Data Set S1. The Unaveraged *S. pombe* E-MAP in Tab-Delimited Format

Data Set S2. The Averaged *S. pombe* E-MAP in Tab-Delimited Text Format

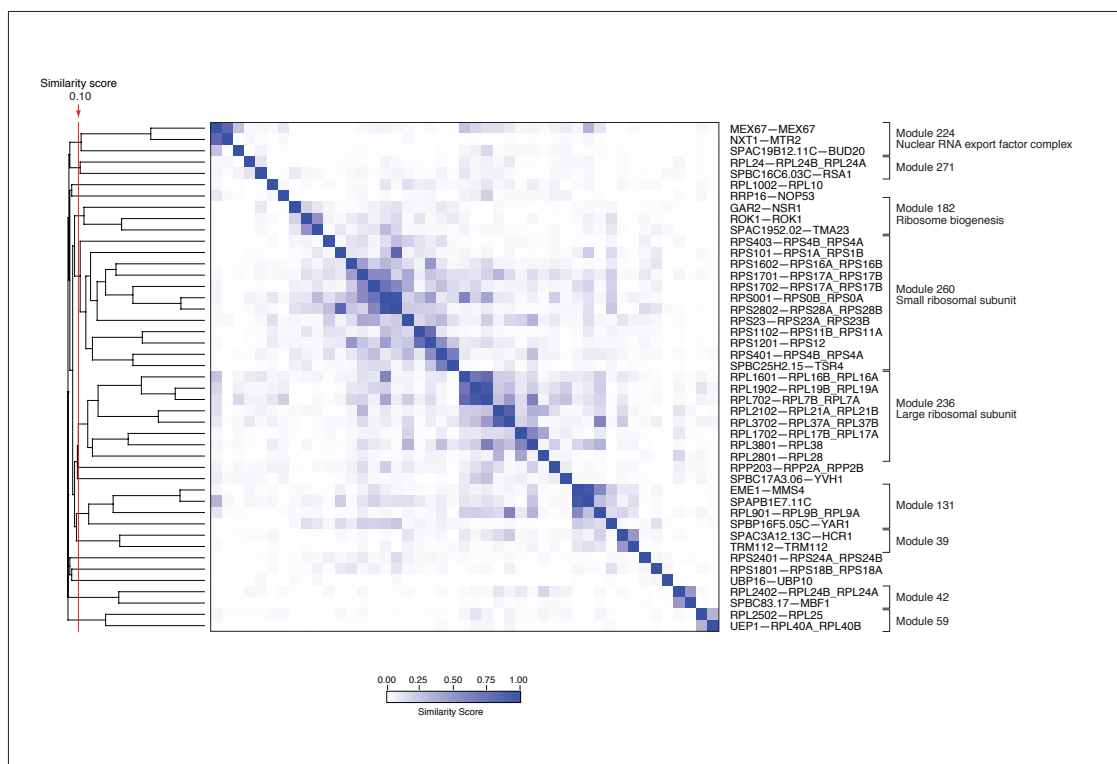
Data Set S3. The Similarity Scores for Every Gene Pair in the *S. pombe* E-MAP

Data Set S4. The Scaled and Merged E-Map AND SGA *S. cerevisiae* Data

Table S4. Query genes relevant to TOR biology in *S. pombe* screen

| Gene | Function |
|-------------|----------------------------------------------------------------------------|
| tor2-DAmP | ser/thr kinase, TORC1 |
| tor1 | ser/thr kinase, TORC2 |
| wat1 | LST8; WD repeat, polarized cell growth, TORC1, TORC2 |
| mip1 | Raptor; guanine binding protein, mei2 driven meiosis, TORC1 |
| toc1 | PRAS40; unknown function, TORC1 |
| rhb1 | Rheb; GTPase binds TORC1 |
| tco89 | TORC1 component |
| fkh1 | FKBP12; required for efficient mating, binds FK506 and rapamycin, TORC1 |
| tel2 | DNA replication checkpoint, TORC1, TORC2 (aka rad5) |
| cka1 | casein kinase II, component of TORC1, TORC2 |
| Sin1 | interacts with stress-activated MAP kinase sty1, stress response, TORC2 |
| bit61 | unknown function, TORC2 |
| tsc1 | amino acid uptake, represses TORC1 |
| tsc2 | amino acid uptake, represses TORC1 |
| gad8 | AKT; ser/thr kinase, AGC kinase, nitrogen sensitive, activates TORC1 |
| ppk21 | protein kinase (PDK1 homolog) |
| ksg1 | kinase for sporulation and growth, phosphorylates pka1 T356 (PDK1 homolog) |
| sck2 | S6K; serine/threonine kinase |
| its3 | PI 4-phosphate 5-kinase, regulates cytokinesis |
| mei4 | meiosis transcription factor interacts with fkh1 |
| byr1 | MAPKK upstream of Spk1 |
| rad24 | 14-3-3 protein interacts with byr and mei proteins |
| vps34/pi3k | PI3K kinase, stress tolerance |
| ptn1 | PTEN; phosphatase |
| cdr2 | ser/thr kinase, cell cycle progression, nitrogen sensitive |
| sty1 | MAPK stress signals, nitrogen starvation response |
| SPAC513.07 | unknown function; annotated TOR interacting from 2hybrid screen |
| toll | torc1 (target of lithium), monophosphatase, salt stress |
| upf2 | regulates nonsense mediated decay, oxidative stress |
| SPAC607.04 | inositol polyphosphate kinase family (ipk2) |
| fab1 | PI-3-P 5-kinase |
| SPAC824.01 | PI 3-,4-kinase, actin organization |
| pik1 | PI 4-kinase, cytokinesis |
| SPBC577.06c | PIK |
| gsk3 | ser/thr kinase gsk3 |
| fh1 | forkhead transcription protein |
| efc25 | GEF regulates cell morphology |
| tip41 | nitrogen response via type 2A phosphatase |
| isp6 | serine protease; protein degradation during nitrogen starvation |

Supplemental Figures



Supplementary Figure 3

Figure S1. Hierarchical modularity of ribosomal biogenesis

The tree is cut at a threshold (red line) to identify disjoint modules (labeled along the right hand side of the figure). This figure also serves as an example of hierarchical modularity – modules 236 and 260 contain members of the large and small ribosomal subunits. However, cutting the tree at a lower similarity score results in these two modules being merged into a single ‘ribosomal module’. Indeed the whole section of the tree can be considered a module, containing genes involved in translation and ribosome biogenesis.

Appendix B: Chapter 3 Supplemental

Supplemental Tables

Available online (<http://cellreports.cell.com/>; Kliegman et al. (2013) supplemental information)

Table S1. Dose-dependent changes in response to RAPA or BEZ

Table S2. Genes with measurements at all drug concentrations

Table S3. Metabolite levels over time course drug treatment

Table S4. Queries used for statistical averaging

Table S5. Strains used in this Study

Supplemental Figures

| Compound | wt-TOR2 halo | as-TOR2 halo | wt-MEC1 halo | as-MEC1 halo |
|----------------|--------------|--------------|--------------|--------------|
| DMSO | - | - | - | - |
| PI-121 | - | - | n/a | n/a |
| INK1232 | - | - | n/a | n/a |
| INK128 | - | - | n/a | n/a |
| PI-103 | - | - | n/a | n/a |
| LY29223 | - | - | n/a | n/a |
| LY29223-ETHYL | - | - | n/a | n/a |
| LY29223-METHYL | - | - | n/a | n/a |
| LY29223-PROPYL | - | - | n/a | n/a |
| LY29223-iPr | - | - | n/a | n/a |
| LY29223-phenyl | - | - | n/a | n/a |
| LY29223-BUTYL | - | - | n/a | n/a |
| LY29223-BENZYL | - | - | n/a | n/a |
| BEZ235 | - | + | - | + |
| 3MB-PP1 | - | - | - | - |
| 3IB-PP1 | - | - | - | - |
| 3BR-PP1 | - | - | - | - |
| STAR12 | - | - | - | - |
| STAR26 | - | - | - | - |
| AQ201 | - | - | - | - |
| AQ206 | - | - | - | - |
| FUR164 | - | - | - | - |
| FUR174 | - | - | - | - |
| DR042 | - | - | - | - |
| CZ02 | - | - | - | - |
| 1NM-PP1 | - | - | n/a | n/a |
| 2NM-PP1 | - | - | n/a | n/a |
| CZ22 | - | - | n/a | n/a |
| BA30 | - | - | n/a | n/a |
| BA50 | - | - | n/a | n/a |
| BA121 | - | - | n/a | n/a |
| BA146 | - | - | n/a | n/a |
| PP242 | - | - | n/a | n/a |
| ZK325 | - | - | n/a | n/a |
| ZK327 | - | - | n/a | n/a |
| RAPA | + | + | + | + |

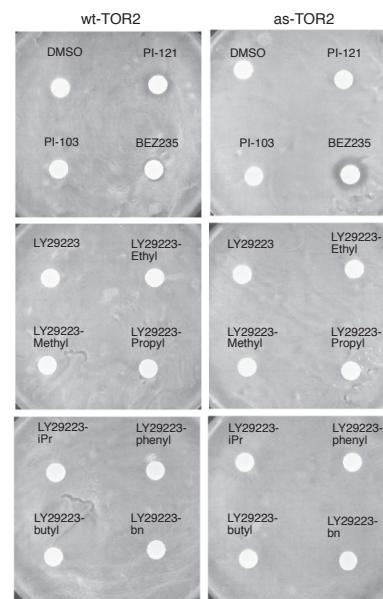


Figure S2. Compounds screened against as-alleles

The wt-TOR2, as-TOR2, wt-MEC1, and as-MEC1 for selectivity against the analog-sensitive allele. (+) indicates sensitivity, (-) indicates insensitivity. (n/a) indicates the compound was not screened. The images show an example of screened plates.

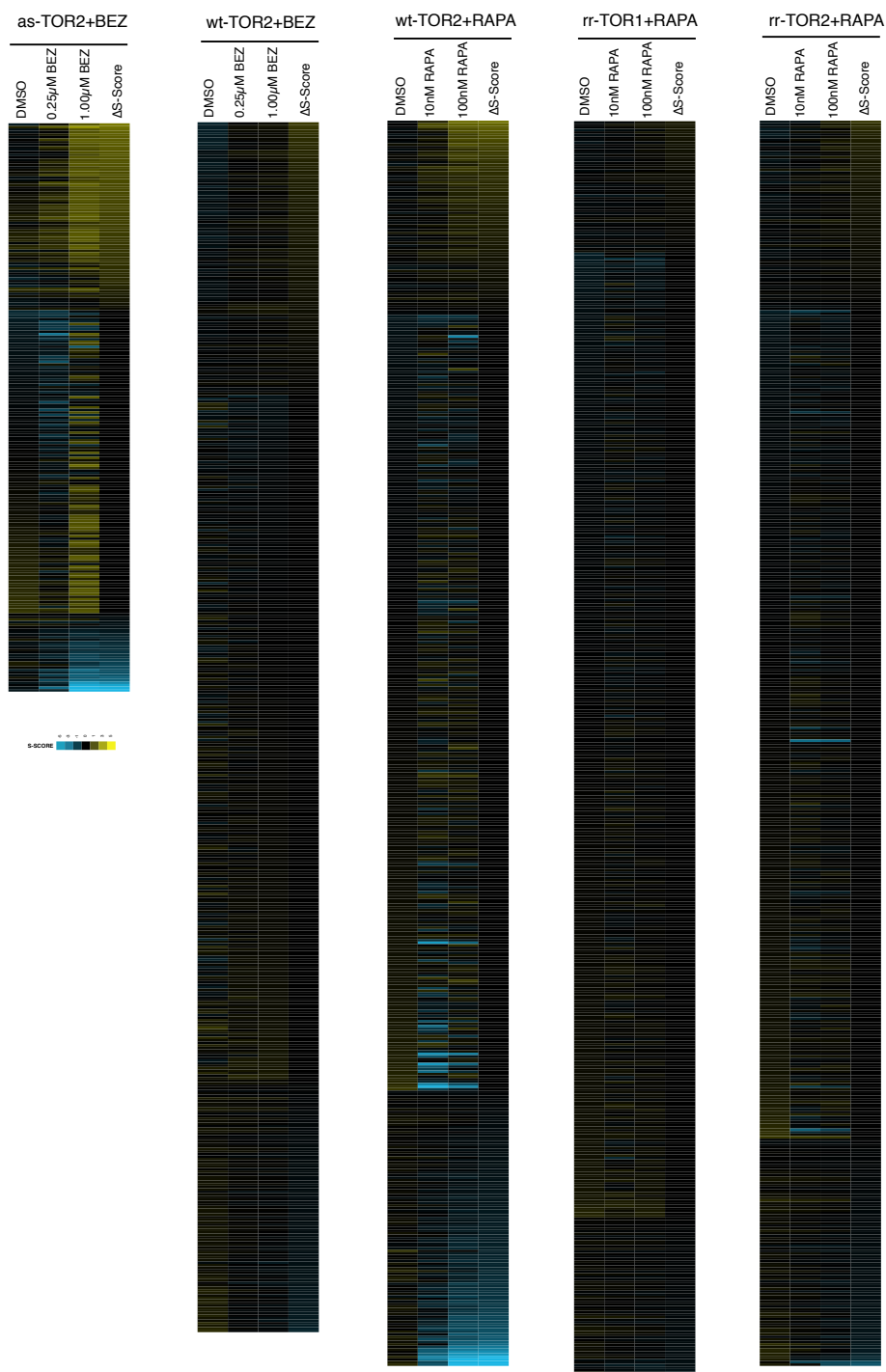


Figure S3. Total Dose-Dependent ChE-MAP

Shown with corresponding Δ S-scores (related to Figure 2). All dose-dependent genetic interactions (including controls) collected and used for analysis including Δ S-scores.

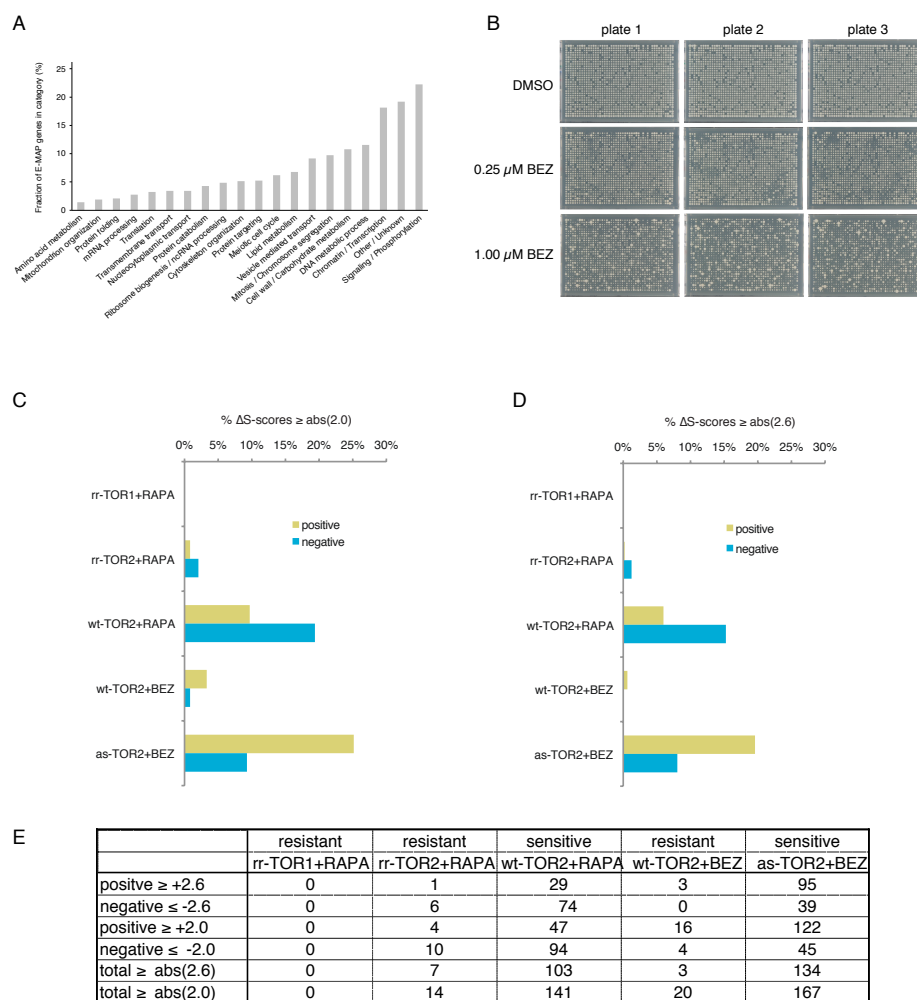


Figure S4. ChEMAP parameters, plate pictures, and quantification

(A) Fraction of ChE-MAP genes in each category by percent of total genes on array. (B) Representative plate pictures of double mutant colonies at different doses of BEZ235 after 24 hours growth at 30°C. (C) Positive and negative hits for resistant and sensitive datasets using a threshold of ΔS -score $\geq \text{abs}(2.0)$. (D) Positive and negative hits for resistant and sensitive datasets using a threshold of ΔS -score $\geq \text{abs}(2.6)$. (E) Number of positive and negative hits at specified threshold for resistant and sensitive datasets

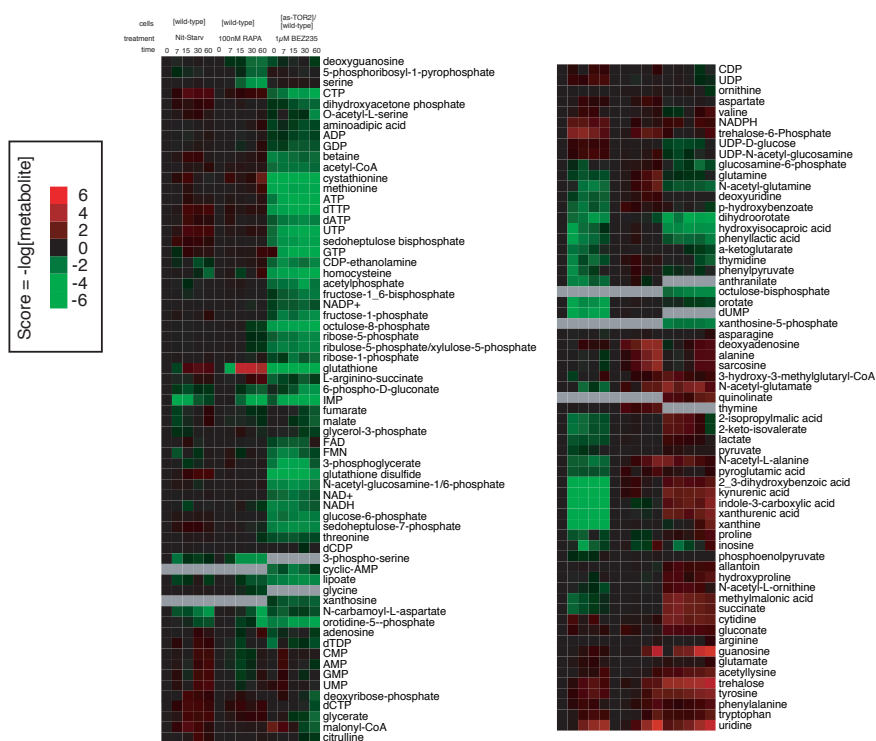


Figure S5. Regulation of metabolites

Heatmap showing downregulation (green) and upregulation (red) of metabolites upon nitrogen-starvation (wt-TOR2), treatment with rapamycin (wt-TOR2), or BEZ235 (as-TOR2). Metabolite levels for as-TOR2 is normalized vs. wild-type treated with drug at every time point during the experiment.

Bibliography

- (null), (null), (null), Tamanoi, F., and (null) (2008). Fission yeast TOR complex 2 activates the AGC-family Gad8 kinase essential for stress resistance and cell cycle control. *Cell Cycle* 7, 358–364.
- Aguilar, P.S., Fröhlich, F., Rehman, M., Shales, M., Ulitsky, I., Olivera-Couto, A., Braberg, H., Shamir, R., Walter, P., Mann, M., et al. (2010). A plasma-membrane E-MAP reveals links of the eisosome with sphingolipid metabolism and endosomal trafficking. *Nat Struct Mol Biol* 17, 901–908.
- Ahmad, T., and Eisen, T. (2004). Kinase inhibition with BAY 43-9006 in renal cell carcinoma. *Clin. Cancer Res.* 10, 6388S–92S.
- Alaimo, P.J., Knight, Z.A., and Shokat, K.M. (2005). Targeting the gatekeeper residue in phosphoinositide 3-kinases. *Bioorg Med Chem* 13, 2825–2836.
- Aronova, S., Wedaman, K., Aronov, P.A., Fontes, K., Ramos, K., Hammock, B.D., and Powers, T. (2008). Regulation of ceramide biosynthesis by TOR complex 2. *Cell Metab* 7, 148–158.
- Babu, M., Díaz-Mejía, J.J., Vlasblom, J., Gagarinova, A., Phanse, S., Graham, C., Yousif, F., Ding, H., Xiong, X., Nazarians-Armavil, A., et al. (2011). Genetic interaction maps in *Escherichia coli* reveal functional crosstalk among cell envelope biogenesis pathways. *PLoS Genet.* 7, e1002377.
- Bandyopadhyay, S., Kelley, R., Krogan, N.J., and Ideker, T. (2008). Functional maps of protein complexes from quantitative genetic interaction data. *PLoS Comput. Biol.* 4, e1000065.
- Bandyopadhyay, S., Mehta, M., Kuo, D., Sung, M.-K., Chuang, R., Jaehnig, E.J., Bodenmiller, B., Licon, K., Copeland, W., Shales, M., et al. (2010). Rewiring of genetic networks in response to DNA damage. *Science* 330, 1385–1389.
- Baryshnikova, A., Costanzo, M., Kim, Y., Ding, H., Koh, J., Toufighi, K., Youn, J.-Y., Ou, J., San Luis, B.-J., Bandyopadhyay, S., et al. (2010). Quantitative analysis of fitness and genetic interactions in yeast on a genome scale. *Nat Methods* 7, 1017–1024.

Beeler, T., Bacikova, D., Gable, K., Hopkins, L., Johnson, C., Slife, H., and Dunn, T. (1998). The *Saccharomyces cerevisiae* TSC10/YBR265w gene encoding 3-ketosphinganine reductase is identified in a screen for temperature-sensitive suppressors of the Ca²⁺-sensitive *csg2Delta* mutant. *J Biol Chem* 273, 30688–30694.

Beltrao, P., Cagney, G., and Krogan, N.J. (2010). Quantitative genetic interactions reveal biological modularity. *Cell* 141, 739–745.

Berchtold, D., and Walther, T.C. (2009). TORC2 plasma membrane localization is essential for cell viability and restricted to a distinct domain. *Mol Biol Cell* 20, 1565–1575.

Berchtold, D., Piccolis, M., Chiaruttini, N., Riezman, I., Riezman, H., Roux, A., Walther, T.C., and Loewith, R. (2012). Plasma membrane stress induces relocalization of Slm proteins and activation of TORC2 to promote sphingolipid synthesis. *Nat Cell Biol* 14, 542–547.

Bishop, A.C., Ubersax, J.A., Petsch, D.T., Matheos, D.P., Gray, N.S., Blethrow, J., Shimizu, E., Tsien, J.Z., Schultz, P.G., Rose, M.D., et al. (2000). A chemical switch for inhibitor-sensitive alleles of any protein kinase. *Nature* 407, 395–401.

Boss, D.S., Beijnen, J.H., and Schellens, J.H.M. (2009). Clinical experience with aurora kinase inhibitors: a review. *Oncologist* 14, 780–793.

Boulbés, D.R., Shaiken, T., and Sarbassov, D.D. (2011). Endoplasmic reticulum is a main localization site of mTORC2. *Biochem Biophys Res Commun* 413, 46–52.

Breslow, D.K., Cameron, D.M., Collins, S.R., Schuldiner, M., Stewart-Ornstein, J., Newman, H.W., Braun, S., Madhani, H.D., Krogan, N.J., and Weissman, J.S. (2008). A comprehensive strategy enabling high-resolution functional analysis of the yeast genome. *Nat Methods* 5, 711–718.

Breslow, D.K., Collins, S.R., Bodenmiller, B., Aebersold, R., Simons, K., Shevchenko, A., Ejsing, C.S., and Weissman, J.S. (2010). Orm family proteins mediate sphingolipid homeostasis. *Nature* 463, 1048–1053.

Brockman, R.W. (1963). MECHANISMS OF RESISTANCE TO ANTICANCER AGENTS. *Adv. Cancer Res.* 7, 129–234.

- Butland, G., Babu, M., Díaz-Mejía, J.J., Bohdana, F., Phanse, S., Gold, B., Yang, W., Li, J., Gagarinova, A.G., Pogoutse, O., et al. (2008). eSGA: E. coli synthetic genetic array analysis. *Nat Methods* 5, 789–795.
- Buzko, O., and Shokat, K.M. (2002). A kinase sequence database: sequence alignments and family assignment. *Bioinformatics* 18, 1274–1275.
- Byrne, A.B., Weirauch, M.T., Wong, V., Koeva, M., Dixon, S.J., Stuart, J.M., and Roy, P.J. (2007). A global analysis of genetic interactions in *Caenorhabditis elegans*. *J. Biol.* 6, 8.
- Cafferkey, R., Young, P.R., McLaughlin, M.M., Bergsma, D.J., Koltin, Y., Sathe, G.M., Faucette, L., Eng, W.K., Johnson, R.K., and Livi, G.P. (1993). Dominant missense mutations in a novel yeast protein related to mammalian phosphatidylinositol 3-kinase and VPS34 abrogate rapamycin cytotoxicity. *Mol Cell Biol* 13, 6012–6023.
- Capra, J.A., Pollard, K.S., and Singh, M. (2010). Novel genes exhibit distinct patterns of function acquisition and network integration. *Genome Biol* 11, R127.
- Casadio, A., Martin, K.C., Giustetto, M., Zhu, H., Chen, M., Bartsch, D., Bailey, C.H., and Kandel, E.R. (1999). A transient, neuron-wide form of CREB-mediated long-term facilitation can be stabilized at specific synapses by local protein synthesis. *Cell* 99, 221–237.
- Chabner, B.A., and Roberts, T.G. (2005). Timeline: Chemotherapy and the war on cancer. *Nat. Rev. Cancer* 5, 65–72.
- Chen, R., Mias, G.I., Li-Pook-Than, J., Jiang, L., Lam, H.Y.K., Chen, R., Miriami, E., Karczewski, K.J., Hariharan, M., Dewey, F.E., et al. (2012). Personal omics profiling reveals dynamic molecular and medical phenotypes. *Cell* 148, 1293–1307.
- Chung, J., Kuo, C.J., Crabtree, G.R., and Blenis, J. (1992). Rapamycin-FKBP specifically blocks growth-dependent activation of and signaling by the 70 kd S6 protein kinases. *Cell* 69, 1227–1236.
- Clasquin, M.F., Melamud, E., Singer, A., Gooding, J.R., Xu, X., Dong, A., Cui, H., Campagna, S.R., Savchenko, A., Yakunin, A.F., et al. (2011). Riboneogenesis in yeast. *Cell* 145, 969–980.

- Collins, S.R., Miller, K.M., Maas, N.L., Roguev, A., Fillingham, J., Chu, C.S., Schuldiner, M., Gebbia, M., Recht, J., Shales, M., et al. (2007). Functional dissection of protein complexes involved in yeast chromosome biology using a genetic interaction map. *Nature* 446, 806–810.
- Collins, S.R., Roguev, A., and Krogan, N.J. (2010). Quantitative genetic interaction mapping using the E-MAP approach. *Meth Enzymol* 470, 205–231.
- Collins, S.R., Schuldiner, M., Krogan, N.J., and Weissman, J.S. (2006). A strategy for extracting and analyzing large-scale quantitative epistatic interaction data. *Genome Biol* 7, R63.
- Costanzo, M., Baryshnikova, A., Bellay, J., Kim, Y., Spear, E.D., Sevier, C.S., Ding, H., Koh, J.L.Y., Toufighi, K., Mostafavi, S., et al. (2010). The genetic landscape of a cell. *Science* 327, 425–431.
- Dar, A.C., Das, T.K., Shokat, K.M., and Cagan, R.L. (2012). Chemical genetic discovery of targets and anti-targets for cancer polypharmacology. *Nature* 486, 80–84.
- de Bono, J.S., and Ashworth, A. (2010). Translating cancer research into targeted therapeutics. *Nature* 467, 543–549.
- de Bono, J.S., Logothetis, C.J., Molina, A., Fizazi, K., North, S., Chu, L., Chi, K.N., Jones, R.J., Goodman, O.B., Saad, F., et al. (2011). Abiraterone and increased survival in metastatic prostate cancer. *N. Engl. J. Med.* 364, 1995–2005.
- Deberardinis, R.J., Sayed, N., Ditsworth, D., and Thompson, C.B. (2008). Brick by brick: metabolism and tumor cell growth. *Curr Opin Genet Dev* 18, 54–61.
- Dixon, S.J., Fedyshyn, Y., Koh, J.L.Y., Prasad, T.S.K., Chahwan, C., Chua, G., Toufighi, K., Baryshnikova, A., Hayles, J., Hoe, K.-L., et al. (2008). Significant conservation of synthetic lethal genetic interaction networks between distantly related eukaryotes. *Proc Natl Acad Sci USA* 105, 16653–16658.
- Düvel, K., Yecies, J.L., Menon, S., Raman, P., Lipovsky, A.I., Souza, A.L., Triantafellow, E., Ma, Q., Gorski, R., Cleaver, S., et al. (2010). Activation of a metabolic gene regulatory network downstream of mTOR complex 1. *Mol*

Cell 39, 171–183.

Fan, X., Martin-Brown, S., Florens, L., and Li, R. (2008). Intrinsic capability of budding yeast cofilin to promote turnover of tropomyosin-bound actin filaments. *PLoS ONE* 3, e3641.

Fasolo, J., Sboner, A., Sun, M.G.F., Yu, H., Chen, R., Sharon, D., Kim, P.M., Gerstein, M., and Snyder, M. (2011). Diverse protein kinase interactions identified by protein microarrays reveal novel connections between cellular processes. *Genes Dev* 25, 767–778.

Feldman, M.E., Apsel, B., Uotila, A., Loewith, R., Knight, Z.A., Ruggero, D., Shokat, K.M., and Hunter, T. (2009). Active-Site Inhibitors of mTOR Target Rapamycin-Resistant Outputs of mTORC1 and mTORC2. *PLoS Biol* 7, e38.

Fiedler, D., Braberg, H., Mehta, M., (null), Cagney, G., (null), (null), Shales, M., Collins, S.R., (null), et al. (2009). Functional organization of the *S. cerevisiae* phosphorylation network. *Cell* 136, 952–963.

Fleischer, T.C., Weaver, C.M., McAfee, K.J., Jennings, J.L., and Link, A.J. (2006). Systematic identification and functional screens of uncharacterized proteins associated with eukaryotic ribosomal complexes. *Genes Dev* 20, 1294–1307.

Garcia, M.A., Koonruga, N., and Toda, T. (2002). Two kinesin-like Kin I family proteins in fission yeast regulate the establishment of metaphase and the onset of anaphase A. *Curr Biol* 12, 610–621.

Gerlinger, M., Rowan, A.J., Horswell, S., Larkin, J., Endesfelder, D., Gronroos, E., Martinez, P., Matthews, N., Stewart, A., Tarpey, P., et al. (2012). Intratumor heterogeneity and branched evolution revealed by multiregion sequencing. *N. Engl. J. Med.* 366, 883–892.

Giaever, G., Chu, A.M., Ni, L., Connelly, C., Riles, L., Véronneau, S., Dow, S., Lucau-Danila, A., Anderson, K., André, B., et al. (2002). Functional profiling of the *Saccharomyces cerevisiae* genome. *Nature* 418, 387–391.

Graille, M., Meyer, P., Leulliot, N., Sorel, I., Janin, J., Van Tilbeurgh, H., and Quevillon-Cheruel, S. (2005). Crystal structure of the *S. cerevisiae* D-ribose-5-phosphate isomerase: comparison with the archaeal and bacterial enzymes. *Biochimie* 87, 763–769.

- Greaves, M., and Maley, C.C. (2012). Clonal evolution in cancer. *Nature* *481*, 306–313.
- Greenman, C., Stephens, P., Smith, R., Dalgliesh, G.L., Hunter, C., Bignell, G., Davies, H., Teague, J., Butler, A., Stevens, C., et al. (2007). Patterns of somatic mutation in human cancer genomes. *Nature* *446*, 153–158.
- Hannum, G., Srivas, R., Guénolé, A., van Attikum, H., Krogan, N.J., Karp, R.M., and Ideker, T. (2009). Genome-wide association data reveal a global map of genetic interactions among protein complexes. *PLoS Genet.* *5*, e1000782.
- Haura, E.B., Ricart, A.D., Larson, T.G., Stella, P.J., Bazhenova, L., Miller, V.A., Cohen, R.B., Eisenberg, P.D., Selaru, P., Wilner, K.D., et al. (2010). A phase II study of PD-0325901, an oral MEK inhibitor, in previously treated patients with advanced non-small cell lung cancer. *Clin. Cancer Res.* *16*, 2450–2457.
- Hawkins, R.D., Hon, G.C., and Ren, B. (2010). Next-generation genomics: an integrative approach. *Nat. Rev. Genet.* *11*, 476–486.
- Heidorn, S.J., Milagre, C., Whittaker, S., Nourry, A., Niculescu-Duvas, I., Dhomen, N., Hussain, J., Reis-Filho, J.S., Springer, C.J., Pritchard, C., et al. (2010). Kinase-dead BRAF and oncogenic RAS cooperate to drive tumor progression through CRAF. *Cell* *140*, 209–221.
- Heitman, J., Movva, N.R., and Hall, M.N. (1991). Targets for cell cycle arrest by the immunosuppressant rapamycin in yeast. *Science* *253*, 905–909.
- Helliwell, S.B., Howald, I., Barbet, N., and Hall, M.N. (1998a). TOR2 is part of two related signaling pathways coordinating cell growth in *Saccharomyces cerevisiae*. *Genetics* *148*, 99–112.
- Helliwell, S.B., Schmidt, A., Ohya, Y., and Hall, M.N. (1998b). The Rho1 effector Pkc1, but not Bni1, mediates signalling from Tor2 to the actin cytoskeleton. *Curr Biol* *8*, 1211–1214.
- Helliwell, S.B., Wagner, P., Kunz, J., Deuter-Reinhard, M., Henriquez, R., and Hall, M.N. (1994). TOR1 and TOR2 are structurally and functionally similar but not identical phosphatidylinositol kinase homologues in yeast. *Mol Biol Cell* *5*, 105–118.

- Helmlinger, D., Marguerat, S., Villén, J., Gygi, S.P., Bähler, J., and Winston, F. (2008). The *S. pombe* SAGA complex controls the switch from proliferation to sexual differentiation through the opposing roles of its subunits Gcn5 and Spt8. *Genes Dev* 22, 3184–3195.
- Hesselberth, J.R., Miller, J.P., Golob, A., Stajich, J.E., Michaud, G.A., and Fields, S. (2006). Comparative analysis of *Saccharomyces cerevisiae* WW domains and their interacting proteins. *Genome Biol* 7, R30.
- Hoppins, S., Collins, S.R., Cassidy-Stone, A., Hummel, E., Devay, R.M., Lackner, L.L., Westermann, B., Schuldiner, M., Weissman, J.S., and Nunnari, J. (2011). A mitochondrial-focused genetic interaction map reveals a scaffold-like complex required for inner membrane organization in mitochondria. *J Cell Biol* 195, 323–340.
- Horn, T., Sandmann, T., Fischer, B., Axelsson, E., Huber, W., and Boutros, M. (2011). Mapping of signaling networks through synthetic genetic interaction analysis by RNAi. *Nat Methods* 8, 341–346.
- Huang, J., Dibble, C.C., Matsuzaki, M., and Manning, B.D. (2008). The TSC1-TSC2 complex is required for proper activation of mTOR complex 2. *Mol Cell Biol* 28, 4104–4115.
- Iadevaia, S., Lu, Y., Morales, F.C., Mills, G.B., and Ram, P.T. (2010). Identification of optimal drug combinations targeting cellular networks: integrating phospho-proteomics and computational network analysis. *Cancer Res* 70, 6704–6714.
- Inoki, K., Corradetti, M.N., and Guan, K.-L. (2005). Dysregulation of the TSC-mTOR pathway in human disease. *Nat Genet* 37, 19–24.
- Iwaki, T., Giga-Hama, Y., and Takegawa, K. (2006). A survey of all 11 ABC transporters in fission yeast: two novel ABC transporters are required for red pigment accumulation in a *Schizosaccharomyces pombe* adenine biosynthetic mutant. *Microbiology* 152, 2309–2321.
- Kaeberlein, M., Hu, D., Kerr, E.O., Tsuchiya, M., Westman, E.A., Dang, N., Fields, S., and Kennedy, B.K. (2005). Increased life span due to calorie restriction in respiratory-deficient yeast. *PLoS Genet.* 1, e69.
- Kamada, Y., Fujioka, Y., Suzuki, N.N., Inagaki, F., Wullschleger, S., Loewith, R., Hall, M.N., and Ohsumi, Y. (2005). Tor2 directly

phosphorylates the AGC kinase Ypk2 to regulate actin polarization. *Mol Cell Biol* 25, 7239–7248.

Kashtan, N., and Alon, U. (2005). Spontaneous evolution of modularity and network motifs. *Proc Natl Acad Sci USA* 102, 13773–13778.

Keith, C.T., Borisy, A.A., and Stockwell, B.R. (2005). Multicomponent therapeutics for networked systems. *Nat Rev Drug Discov* 4, 71–78.

Kelley, B.P., Sharan, R., Karp, R.M., Sittler, T., Root, D.E., Stockwell, B.R., and Ideker, T. (2003). Conserved pathways within bacteria and yeast as revealed by global protein network alignment. *Proc Natl Acad Sci USA* 100, 11394–11399.

Kelley, R., and Ideker, T. (2005). Systematic interpretation of genetic interactions using protein networks. *Nat Biotechnol* 23, 561–566.

Keogh, M.-C., Kurdistani, S.K., Morris, S.A., Ahn, S.H., Podolny, V., Collins, S.R., Schuldiner, M., Chin, K., Punna, T., Thompson, N.J., et al. (2005). Cotranscriptional set2 methylation of histone H3 lysine 36 recruits a repressive Rpd3 complex. *Cell* 123, 593–605.

Kitano, H. (2010). Violations of robustness trade-offs. *Mol Syst Biol* 6, 384.

Knight, Z.A., Lin, H., and Shokat, K.M. (2010). Targeting the cancer kinome through polypharmacology. 1–8.

Kobor, M.S., Venkatasubrahmanyam, S., Meneghini, M.D., Gin, J.W., Jennings, J.L., Link, A.J., Madhani, H.D., and Rine, J. (2004). A protein complex containing the conserved Swi2/Snf2-related ATPase Swr1p deposits histone variant H2A.Z into euchromatin. *PLoS Biol* 2, E131.

Krogan, N.J., Cagney, G., Yu, H., Zhong, G., Guo, X., Ignatchenko, A., Li, J., Pu, S., Datta, N., Tikuisis, A.P., et al. (2006). Global landscape of protein complexes in the yeast *Saccharomyces cerevisiae*. *Nature* 440, 637–643.

Krogan, N.J., Keogh, M.-C., Datta, N., Sawa, C., Ryan, O.W., Ding, H., Haw, R.A., Pootoolal, J., Tong, A., Canadien, V., et al. (2003). A Snf2 family ATPase complex required for recruitment of the histone H2A variant Htz1. *Mol Cell* 12, 1565–1576.

Lehner, B. (2007). Modelling genotype-phenotype relationships and human

- disease with genetic interaction networks. *J. Exp. Biol.* *210*, 1559–1566.
- Lehner, B., Crombie, C., Tischler, J., Fortunato, A., and Fraser, A.G. (2006). Systematic mapping of genetic interactions in *Caenorhabditis elegans* identifies common modifiers of diverse signaling pathways. *Nature Publishing Group* *38*, 896–903.
- Liu, Q., Ren, T., Fresques, T., Oppliger, W., Niles, B.J., Hur, W., Sabatini, D.M., Hall, M.N., Powers, T., and Gray, N.S. (2012). Selective ATP-Competitive Inhibitors of TOR Suppress Rapamycin-Insensitive Function of TORC2 in *Saccharomyces cerevisiae*. *ACS Chem. Biol.* *7*, 982–987.
- Loewith, R., Jacinto, E., Wullschleger, S., Lorberg, A., Crespo, J.L., Bonenfant, D., Oppliger, W., Jenoe, P., and Hall, M.N. (2002). Two TOR complexes, only one of which is rapamycin sensitive, have distinct roles in cell growth control. *Mol Cell* *10*, 457–468.
- Luo, J., Solimini, N.L., and Elledge, S.J. (2009). Principles of cancer therapy: oncogene and non-oncogene addiction. *Cell* *136*, 823–837.
- Martin, D.E., and Hall, M.N. (2005). The expanding TOR signaling network. *Curr Opin Cell Biol* *17*, 158–166.
- Mestres, J., Gregori-Puigjané, E., Valverde, S., and Solé, R.V. (2009). The topology of drug-target interaction networks: implicit dependence on drug properties and target families. *Mol Biosyst* *5*, 1051–1057.
- Meyer, A.E., Hung, N.J., Yang, P., Johnson, A.W., and Craig, E.A. (2007). The specialized cytosolic J-protein, Jjj1, functions in 60S ribosomal subunit biogenesis. *Proc Natl Acad Sci USA* *104*, 1558–1563.
- Michaut, M., Baryshnikova, A., Costanzo, M., Myers, C.L., Andrews, B.J., Boone, C., and Bader, G.D. (2011). Protein complexes are central in the yeast genetic landscape. *PLoS Comput. Biol.* *7*, e1001092.
- Mizuguchi, G., Shen, X., Landry, J., Wu, W.-H., Sen, S., and Wu, C. (2004). ATP-driven exchange of histone H2AZ variant catalyzed by SWR1 chromatin remodeling complex. *Science* *303*, 343–348.
- Moroney, J., Wheler, J., Hong, D., Naing, A., Falchook, G., Bodurka, D., Coleman, R., Lu, K., Xiao, L., and Kurzrock, R. (2010). Phase I clinical trials in 85 patients with gynecologic cancer: the M. D. Anderson Cancer

Center experience. *Gynecol. Oncol.* *117*, 467–472.

Murakami, H., Goto, D.B., Toda, T., Chen, E.S., Grewal, S.I., Martienssen, R.A., and Yanagida, M. (2007). Ribonuclease activity of Dis3 is required for mitotic progression and provides a possible link between heterochromatin and kinetochore function. *PLoS ONE* *2*, e317.

Niles, B.J., Mogri, H., Hill, A., Vlahakis, A., and Powers, T. (2012). Plasma membrane recruitment and activation of the AGC kinase Ypk1 is mediated by target of rapamycin complex 2 (TORC2) and its effector proteins Slm1 and Slm2. *Proc Natl Acad Sci USA* *109*, 1536–1541.

Parsons, D.W., Wang, T.-L., Samuels, Y., Bardelli, A., Cummins, J.M., DeLong, L., Silliman, N., Ptak, J., Szabo, S., Willson, J.K.V., et al. (2005). Colorectal cancer: mutations in a signalling pathway. *Nature* *436*, 792.

Phillips, P.C. (2008). Epistasis--the essential role of gene interactions in the structure and evolution of genetic systems. *Nat. Rev. Genet.* *9*, 855–867.

Poulikakos, P.I., Zhang, C., Bollag, G., Shokat, K.M., and Rosen, N. (2010). RAF inhibitors transactivate RAF dimers and ERK signalling in cells with wild-type BRAF. *Nature* *464*, 427–430.

Prahallad, A., Sun, C., Huang, S., Di Nicolantonio, F., Salazar, R., Zecchin, D., Beijersbergen, R.L., Bardelli, A., and Bernards, R. (2012). Unresponsiveness of colon cancer to BRAF(V600E) inhibition through feedback activation of EGFR. *Nature* *483*, 100–103.

Price, D.J., Grove, J.R., Calvo, V., Avruch, J., and Bierer, B.E. (1992). Rapamycin-induced inhibition of the 70-kilodalton S6 protein kinase. *Science* *257*, 973–977.

Ptacek, J., Devgan, G., Michaud, G., Zhu, H., Zhu, X., Fasolo, J., Guo, H., Jona, G., Breitkreutz, A., Sopko, R., et al. (2005). Global analysis of protein phosphorylation in yeast. *Nature* *438*, 679–684.

Richardson, C.J., Bröenstrup, M., Fingar, D.C., Jülich, K., Ballif, B.A., Gygi, S., and Blenis, J. (2004). SKAR is a specific target of S6 kinase 1 in cell growth control. *Curr Biol* *14*, 1540–1549.

Robitaille, A.M., Christen, S., Shimobayashi, M., Cornu, M., Fava, L.L., Moes, S., Prescianotto-Baschong, C., Sauer, U., Jenoe, P., and Hall, M.N.

(2013). Quantitative Phosphoproteomics Reveal mTORC1 Activates de Novo Pyrimidine Synthesis. *Science*.

Roelants, F.M., Breslow, D.K., Muir, A., Weissman, J.S., and Thorner, J. (2011). Protein kinase Ypk1 phosphorylates regulatory proteins Orm1 and Orm2 to control sphingolipid homeostasis in *Saccharomyces cerevisiae*. *108*, 19222–19227.

Roelants, F.M., Torrance, P.D., and Thorner, J. (2004). Differential roles of PDK1- and PDK2-phosphorylation sites in the yeast AGC kinases Ypk1, Pkc1 and Sch9. *Microbiology 150*, 3289–3304.

Roguev, A., (null), Weissman, J.S., and Krogan, N.J. (2007). High-throughput genetic interaction mapping in the fission yeast *Schizosaccharomyces pombe*. *Nat Methods 4*, 861–866.

Roguev, A., Bandyopadhyay, S., Zofall, M., Zhang, K., Fischer, T., Collins, S.R., Qu, H., Shales, M., Park, H.-O., Hayles, J., et al. (2008). Conservation and rewiring of functional modules revealed by an epistasis map in fission yeast. *Science 322*, 405–410.

Ryan, C.J., Roguev, A., Patrick, K., Xu, J., Jahari, H., Tong, Z., Beltrao, P., Shales, M., Qu, H., Collins, S.R., et al. (2012). Hierarchical modularity and the evolution of genetic interactomes across species. *Mol Cell 46*, 691–704.

Sanchez-Perez, I., Renwick, S.J., Crawley, K., Karig, I., Buck, V., Meadows, J.C., Franco-Sanchez, A., Fleig, U., Toda, T., and Millar, J.B.A. (2005). The DASH complex and Klp5/Klp6 kinesin coordinate bipolar chromosome attachment in fission yeast. *Embo J 24*, 2931–2943.

Schmidt, A., Bickle, M., Beck, T., and Hall, M.N. (1997). The yeast phosphatidylinositol kinase homolog TOR2 activates RHO1 and RHO2 via the exchange factor ROM2. *Cell 88*, 531–542.

Schuldiner, M., Collins, S.R., Thompson, N.J., Denic, V., Bhamidipati, A., Punna, T., Ihmels, J., Andrews, B., Boone, C., Greenblatt, J.F., et al. (2005). Exploration of the function and organization of the yeast early secretory pathway through an epistatic miniarray profile. *Cell 123*, 507–519.

Schuldiner, M., Collins, S.R., Weissman, J.S., and Krogan, N.J. (2006). Quantitative genetic analysis in *Saccharomyces cerevisiae* using epistatic miniarray profiles (E-MAPs) and its application to chromatin functions.

Methods *40*, 344–352.

Seaman, M.N., McCaffery, J.M., and Emr, S.D. (1998). A membrane coat complex essential for endosome-to-Golgi retrograde transport in yeast. *J Cell Biol* *142*, 665–681.

Sharan, R., and Ideker, T. (2006). Modeling cellular machinery through biological network comparison. *Nat Biotechnol* *24*, 427–433.

Sharan, R., Suthram, S., Kelley, R.M., Kuhn, T., McCuine, S., Uetz, P., Sittler, T., Karp, R.M., and Ideker, T. (2005). Conserved patterns of protein interaction in multiple species. *Proc Natl Acad Sci USA* *102*, 1974–1979.

Shoemaker, R.H. (2006). The NCI60 human tumour cell line anticancer drug screen. *Nat. Rev. Cancer* *6*, 813–823.

Sipiczki, M. (2000). Where does fission yeast sit on the tree of life? *Genome Biol* *1*, REVIEWS1011.

Stark, C., Breitkreutz, B.-J., Chatr-Aryamontri, A., Boucher, L., Oughtred, R., Livstone, M.S., Nixon, J., Van Auken, K., Wang, X., Shi, X., et al. (2011). The BioGRID Interaction Database: 2011 update. *Nucleic Acids Res* *39*, D698–D704.

Stark, C., Breitkreutz, B.-J., Reguly, T., Boucher, L., Breitkreutz, A., and Tyers, M. (2006). BioGRID: a general repository for interaction datasets. *Nucleic Acids Res* *34*, D535–D539.

Sterner, D.E., Lee, J.M., Hardin, S.E., and Greenleaf, A.L. (1995). The yeast carboxyl-terminal repeat domain kinase CTDK-I is a divergent cyclin-cyclin-dependent kinase complex. *Mol Cell Biol* *15*, 5716–5724.

Stuart, J.M., Segal, E., Koller, D., and Kim, S.K. (2003). A gene-coexpression network for global discovery of conserved genetic modules. *Science* *302*, 249–255.

Sun, S.-Y., Rosenberg, L.M., Wang, X., Zhou, Z., Yue, P., Fu, H., and Khuri, F.R. (2005). Activation of Akt and eIF4E survival pathways by rapamycin-mediated mammalian target of rapamycin inhibition. *Cancer Res* *65*, 7052–7058.

Sun, Y., Miao, Y., Yamane, Y., Zhang, C., Shokat, K.M., Takematsu, H.,

- Kozutsumi, Y., and Drubin, D.G. (2012). Orm protein phosphoregulation mediates transient sphingolipid biosynthesis response to heat stress via the Pkh-Ypk and Cdc55-PP2A pathways. *Mol Biol Cell* 23, 2388–2398.
- Sunnerhagen, P., and Piskur, J. (2010). *Comparative Genomics* (Springer).
- Tabuchi, M., Audhya, A., Parsons, A.B., Boone, C., and Emr, S.D. (2006). The phosphatidylinositol 4,5-bisphosphate and TORC2 binding proteins Slm1 and Slm2 function in sphingolipid regulation. *Mol Cell Biol* 26, 5861–5875.
- Tan, K., Shlomi, T., Feizi, H., Ideker, T., and Sharan, R. (2007). Transcriptional regulation of protein complexes within and across species. *Proc Natl Acad Sci USA* 104, 1283–1288.
- Tang, Z., Luca, M., Portillio, J., Ngo, B., Chang, C., Wen, T., Murray, J., and Carr, A. (2011). LAMMER kinase Kic1 is involved in pre-mRNA processing. *Exp. Cell Res.* 317, 2308–2320.
- Tee, A.R., and Blenis, J. (2005). mTOR, translational control and human disease. *Semin. Cell Dev. Biol.* 16, 29–37.
- The Cancer Genome Atlas Research Network, Analysis working group: Baylor College of Medicine, Creighton, C.J., Morgan, M., Gunaratne, P.H., Wheeler, D.A., Gibbs, R.A., BC Cancer Agency, Gordon Robertson, A., Chu, A., et al. (2013). Comprehensive molecular characterization of clear cell renal cell carcinoma. *Nature*.
- Tischler, J., Lehner, B., and Fraser, A.G. (2008). Evolutionary plasticity of genetic interaction networks. *Nat Genet* 40, 390–391.
- Tischmeyer, W., Schicknick, H., Kraus, M., Seidenbecher, C.I., Staak, S., Scheich, H., and Gundelfinger, E.D. (2003). Rapamycin-sensitive signalling in long-term consolidation of auditory cortex-dependent memory. *Eur J Neurosci* 18, 942–950.
- Tong, A.H.Y., Lesage, G., Bader, G.D., Ding, H., Xu, H., Xin, X., Young, J., Berriz, G.F., Brost, R.L., Chang, M., et al. (2004). Global mapping of the yeast genetic interaction network. *Science* 303, 808–813.
- Typas, A., Nichols, R.J., Siegele, D.A., Shales, M., Collins, S.R., Lim, B., Braberg, H., Yamamoto, N., Takeuchi, R., Wanner, B.L., et al. (2008).

High-throughput, quantitative analyses of genetic interactions in *E. coli*. *Nat Methods* 5, 781–787.

Urban, J., Soulard, A., Huber, A., Lippman, S., Mukhopadhyay, D., Deloche, O., Wanke, V., Anrather, D., Ammerer, G., Riezman, H., et al. (2007). Sch9 Is a Major Target of TORC1 in *Saccharomyces cerevisiae*. *Mol Cell* 26, 663–674.

van Dam, T.J.P., and Snel, B. (2008). Protein complex evolution does not involve extensive network rewiring. *PLoS Comput. Biol.* 4, e1000132.

Wilhelm, S., Carter, C., Lynch, M., Lowinger, T., Dumas, J., Smith, R.A., Schwartz, B., Simantov, R., and Kelley, S. (2006). Discovery and development of sorafenib: a multikinase inhibitor for treating cancer. *Nat Rev Drug Discov* 5, 835–844.

Wilmes, G.M., Bergkessel, M., Bandyopadhyay, S., Shales, M., Braberg, H., Cagney, G., Collins, S.R., Whitworth, G.B., Kress, T.L., Weissman, J.S., et al. (2008). A genetic interaction map of RNA-processing factors reveals links between Sem1/Dss1-containing complexes and mRNA export and splicing. *Mol Cell* 32, 735–746.

Wood, L.D., Parsons, D.W., Jones, S., Lin, J., Sjöblom, T., Leary, R.J., Shen, D., Boca, S.M., Barber, T., Ptak, J., et al. (2007). The genomic landscapes of human breast and colorectal cancers. *Science* 318, 1108–1113.

Xu, Y.-F., Zhao, X., Glass, D.S., Absalan, F., Perlman, D.H., Broach, J.R., and Rabinowitz, J.D. (2012). Regulation of yeast pyruvate kinase by ultrasensitive allostery independent of phosphorylation. *Mol Cell* 48, 52–62.

Yap, T.A., and Workman, P. (2012). Exploiting the cancer genome: strategies for the discovery and clinical development of targeted molecular therapeutics. *Annu. Rev. Pharmacol. Toxicol.* 52, 549–573.

Yu, H., Braun, P., Yildirim, M.A., Lemmens, I., Venkatesan, K., Sahalie, J., Hirozane-Kishikawa, T., Gebreab, F., Li, N., Simonis, N., et al. (2008). High-quality binary protein interaction map of the yeast interactome network. *Science* 322, 104–110.

Yu, Y., Yoon, S.-O., Poulgiannis, G., Yang, Q., Ma, X.M., Villén, J., Kubica, N., Hoffman, G.R., Cantley, L.C., Gygi, S.P., et al. (2011). Phosphoproteomic analysis identifies Grb10 as an mTORC1 substrate that

negatively regulates insulin signaling. *Science* 332, 1322–1326.

Zheng, J., Benschop, J.J., Shales, M., Kemmeren, P., Greenblatt, J., Cagney, G., Holstege, F., Li, H., and Krogan, N.J. (2010). Epistatic relationships reveal the functional organization of yeast transcription factors. *Mol Syst Biol* 6, 420.


Zinzalla, V., Stracka, D., Oppliger, W., and Hall, M.N. (2011). Activation of mTORC2 by association with the ribosome. *Cell* 144, 757–768.

Zoncu, R., Bar-Peled, L., Efeyan, A., Wang, S., Sancak, Y., and Sabatini, D.M. (2011). mTORC1 senses lysosomal amino acids through an inside-out mechanism that requires the vacuolar H(+)-ATPase. *Science* 334, 678–683.

Publishing Agreement

It is the policy of the University to encourage the distribution of all theses, dissertations, and manuscripts. Copies of all UCSF theses, dissertations, and manuscripts will be routed to the library via the Graduate Division. The library will make all theses, dissertations, and manuscripts accessible to the public and will preserve these to the best of their abilities, in perpetuity.

I hereby grant permission to the Graduate Division of the University of California, San Francisco to release copies of my thesis, dissertation, or manuscript to the Campus Library to provide access and preservation, in whole or in part, in perpetuity.



Author Signature

9/5/2013
Date